The Shape of the Main Thermocline

RICK SALMON

Scripps Institution of Oceanography (A-025), La Jolla, CA 92093

(Manuscript received 5 January 1982, in final form 19 July 1982)

ABSTRACT

The mean ocean density field resembles the state of maximum entropy with given values for the upper water mass, total energy and potential enstrophy. Numerical experiments confirm that the thermocline of a freely evolving two-layer model spontaneously assumes the observed double-lobe shape.

1. Introduction

The large-scale density structure of the ocean has not been adequately explained from first physical principles. This paper proposes an explanation for its most salient characteristic: the double-lobed, equatorially symmetric shape of mean isopycnals in the so-called "main thermocline," the thin region of large vertical density gradient that separates the lightest surface waters from the denser waters that compose most of the ocean volume. A century of oceanographic observations has established that the main thermocline has the shape shown schematically in Fig. 1a, with a 400 m minimum in depth on the equator and maxima of roughly 700 m at ±30° latitude. The thermocline intersects the ocean surface at ±50° latitude, and poleward of this intersection the dense lower water contacts the atmosphere directly. Fig. 2 contains north–south density sections based on 25 years of hydrographic data for the three major oceans. These observations show that the two-layer model is a considerable idealization,[1] but the isopycnal shape described above is present in every hemisphere of Fig. 2.

The present study addresses the dynamics of a fluid system composed of two immiscible layers with different constant densities separated by a sharp boundary, which represents the thermocline. The real ocean has often been compared to such a fluid. My principal conclusion concerns the behaviour of the two-layer model in the absence of friction and external forcing: I find that if a blob of low-density fluid is placed at random on the surface of a higher density fluid in a coordinate frame whose vertical rotation rate increases in one direction, then the blob gradually assumes a shape like one of those in Fig. 1, and that the shape is a "maximum likelihood configuration" by the rules of equilibrium statistical mechanics. In uniformly rotating coordinates, the equatorial minimum in thermocline depth is always lacking. In non-rotating coordinates, the blob spreads indefinitely.

While the complete theory relies on the machinery of statistical mechanics, the equilibrium shape can be understood heuristically as the state of most nearly uniform average potential vorticity that total energy conservation will allow. For simplicity, let the model ocean be infinite in the x-direction so that statistical averages are independent of x. If the motion is hydrostatic, then the potential vorticity

$$\left(\frac{\partial v}{\partial x} - \frac{\partial u}{\partial y} + \beta y\right)h^{-1} \tag{1.1}$$

is conserved following the horizontal motions of the fluid columns. Here (u, v) is the (east, north) velocity in the blob, h the thermocline depth, and βy models the northward increase of planetary vorticity, with β a constant. This notation is standard, but it will be explained more fully below. Now if the potential vorticity mixes to a uniform average, and if the average of the quotient can be approximated by the quotient of averages, then

$$-\frac{\partial\langle u\rangle}{\partial y} + \beta y = Q_0\langle h\rangle, \tag{1.2}$$

where Q_0 is the constant value of average potential vorticity. Finally, if the average motion is everywhere geostrophic, and vanishingly small below the thermocline, then

$$\langle u\rangle = -\frac{g'}{\beta y}\frac{d\langle h\rangle}{dy}, \tag{1.3}$$

with g' the "reduced gravity," and (1.2) becomes

$$\frac{d}{dy}\left(\frac{g'}{\beta y}\frac{d\langle h\rangle}{dy}\right) + \beta y = Q_0\langle h\rangle, \tag{1.4}$$

[1] Note, however, that the contour interval in Fig. 2 varies considerably. For a complete discussion of the observations shown, refer to Lynn and Reid (1968).

0022-3670/82/121458-22$09.50

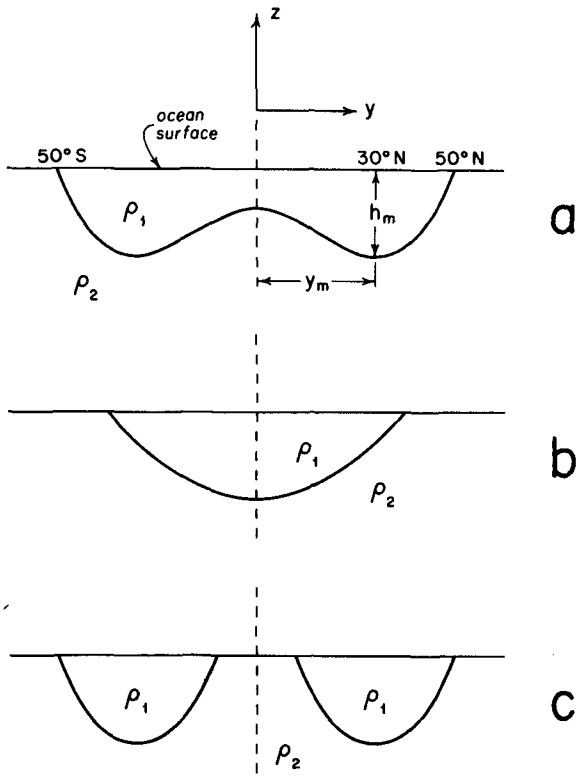

FIG. 1. The main thermocline, which separates warm water with density ρ_1 from colder water with density ρ_2, has the shape shown schematically in (a). For explanation of (b) and (c), refer to the text.

which is an ordinary differential equation for the average thermocline depth $\langle h \rangle$.

The object in this introductory section is not to justify the assumptions leading up to (1.4), but to examine their consequences. The general solution to (1.4) is expansible in a power series about $y = 0$, namely,

$$\langle h \rangle = A + By^2 + ACy^3/3 - (\beta^2/8g')y^4 + BCy^5/15 + ACy^6/72 + \cdots, \quad (1.5)$$

where A and B are the two constants of integration and $C = Q_0\beta/g'$. This solution is symmetric about $y = 0$ only if $Q_0 = 0$ in which case (1.5) reduces to the simple quartic

$$\langle h \rangle = h_m[1 - (y^2 - y_m^2)^2/8r_e^4], \quad (1.6)$$

where now h_m and y_m^2 are the integration constants and

$$r_e = \left(\frac{g'h_m}{\beta^2}\right)^{1/4}. \quad (1.7)$$

The quartic solution (1.6) is single-lobed (Fig. 1b) if $y_m^2 < 0$, double-lobed (Fig. 1a) with maximum depth h_m at $y = \pm y_m$ if $y_m^2 > 0$, and disconnected (Fig. 1c) if $y_m^2 > \sqrt{8}r_e^2$. However, it is impossible to choose h_m and y_m^2 to fit the observations quoted in the first paragraph of this paper. This is expected, because (1.4) with $Q_0 = 0$ equates the magnitudes of the relative and planetary vorticity, whereas the observed ratio of the former to the latter (the Rossby number) is very small. This discrepancy does not by itself disqualify the hypothesis of uniform average potential vorticity, because the putative equilibrium shape would be reached only after friction and external forces have been turned off. A more serious difficulty is that no choice of h_m and y_m^2 can simultaneously give realistic values for the total mass and energy of the blob. Then since the mass and energy are constants of the motion, no realistic initial state can evolve to the shape (1.6).

The impossibility of fitting realistic mass and energy with (1.6) is obvious without elaborate algebra. According to (1.6), the latitudinal width of the blob is of order of the equatorial deformation radius r_e, which is only about 500 km for typical values of g', β and h_m. Thus the blob must be extremely deep to accommodate a realistic mass, and the energy stored in the steeply sloping thermocline of a narrow, relatively deep blob is unrealistically large. (Of course the ocean bottom puts an independent limit on the maximum depth of the blob.)

In this paper, I suggest that the observed main thermocline shape is actually a compromise between the *tendency* toward complete mixing of potential vorticity and the *constraints* to conserve mass and energy. The energy conservation strongly resists complete mixing of potential vorticity, but the mixing proceeds far enough to produce a bimodal thermocline shape. The result is a greatly "subdued" version of (1.6) which retains the bimodality of the quartic solution, but whose latitudinal width is far greater than an equatorial deformation radius.

I support the foregoing interpretation with results from two quite independent investigations. The first is a calculation of the equilibrium thermocline shape using the methods of statistical mechanics. In a suitable phase space for the system, I show that Liouville's theorem holds. Then the equilibrium thermocline configuration is the average over the intersection of phase space manifolds corresponding to fixed values of selected constants of the motion. If the mass and potential enstrophy[2] are the only constants of motion considered, then the equilibrium state has a nearly uniform potential vorticity and the average thermocline shape is close to the quartic solution (1.6) with h_m and y_m^2 chosen to match the prescribed mass and enstrophy. If, more realistically, the mass, potential enstrophy *and* the total energy are used as constants of the motion, then the equilibrium thermocline is like that described in the preceding paragraph.

[2] The space-average squared potential vorticity.

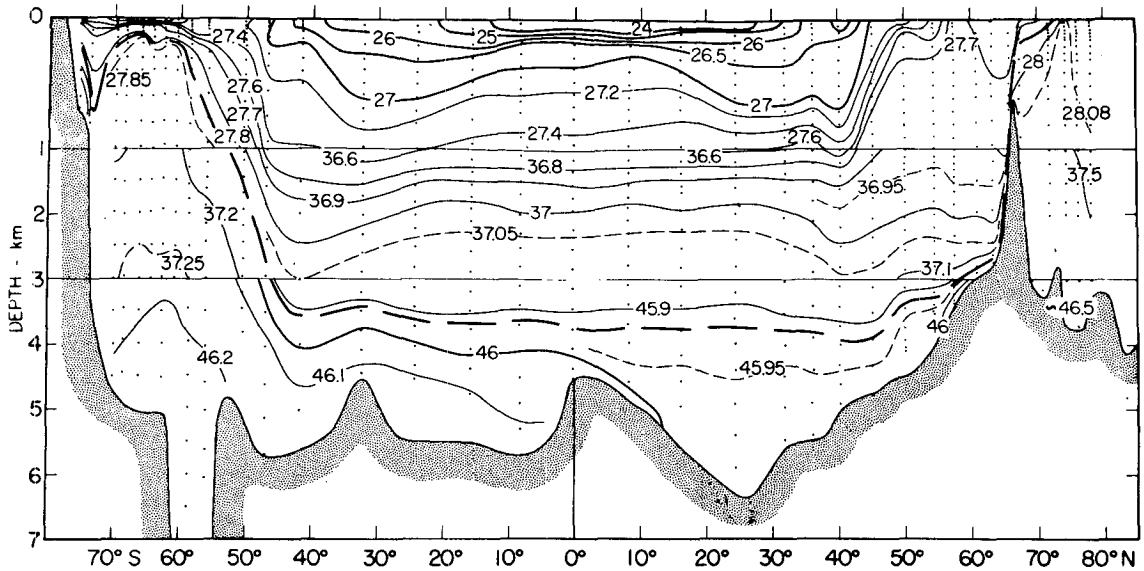
DEPTH - km
0
1
2
3
4
5
6
7
70° S 60° 50° 40° 30° 20° 10° 0° 10° 20° 30° 40° 50° 60° 70° 80° N
27.4
26
25
24
26.5
26
27.7
28
27.85
27.6
27.7
27.8
27
27.2
27
28.08
27.4
27.6
36.6
36.8
36.6
37.5
36.9
36.95
37.2
37
37.05
37.25
37.1
45.9
46.5
46
46.2
46
46.1
45.95

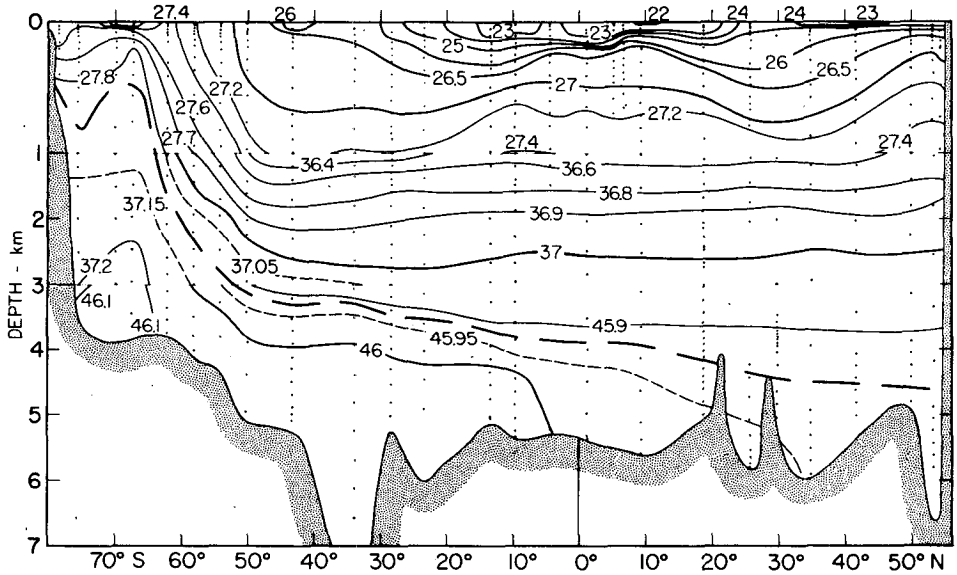
DEPTH - km
0
1
2
3
4
5
6
7
70° S 60° 50° 40° 30° 20° 10° 0° 10° 20° 30° 40° 50° N
27.4
26
25
24
24
23
27.8
27.2
27.6
26.5
27
26
26.5
27.7
27.2
27.4
27.4
36.4
36.6
36.8
37.15
36.9
37
37.2
37.05
46.1
46.1
45.95
45.9
46

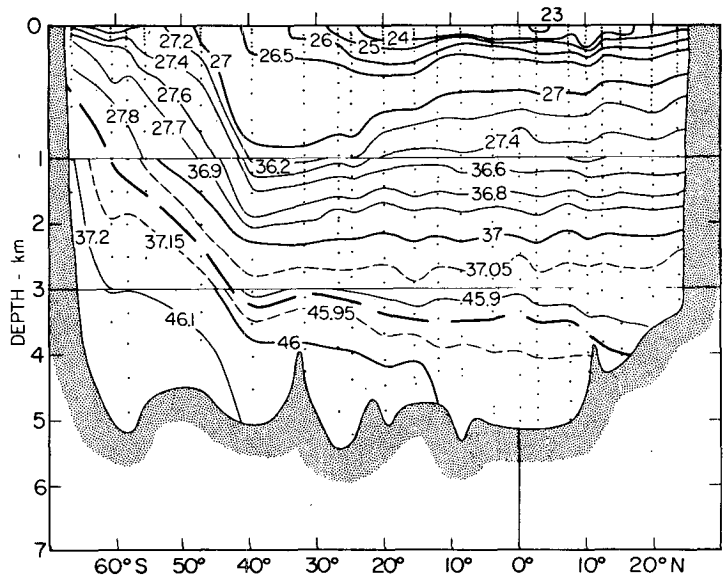
DEPTH - km
0
1
2
3
4
5
6
7
60° S 50° 40° 30° 20° 10° 0° 10° 20° N
23
27.2
26
24
27.4
27
26.5
25
27.6
27
27.8
27.7
27.4
36.9
36.2
36.6
36.8
37.2
37.15
37
37.05
45.9
46.1
45.95
46

The second investigation uses a finite-element numerical model of the blob. The model dynamics are entirely equivalent to the familiar "shallow water" equations of motion, but they are based upon the appropriate form of Hamilton's principle, and the Rayleigh-Ritz procedure. The numerical experiments confirm that a freely evolving blob spontaneously assumes the double-lobe shape, and that, in particular, wind forcing is unnecessary to explain the deepening of the thermocline in mid-latitude.

This paper assumes no special knowledge of oceanography or statistical mechanics. Section 2 defines the two-fluid system and derives its conservation laws. The derivation is nonstandard in that Hamilton's principle provides the dynamical equations, and the conservation of potential vorticity is obtained from Noether's theorem and a symmetry property of the Lagrangian. The Hamiltonian formulation of the dynamics is the basis for the numerical model in Section 5, but readers who are familiar with potential vorticity conservation can skip Section 2 at first reading. Section 3 reviews the basic principles of statistical mechanics in the form required for application to a continuum. Readers who are acquainted with the previous applications of equilibrium statistical mechanics to the macroscopic motions of fluids can skip Section 3. Section 4 extends the statistical theory to cover the blob. The extension is nontrivial, and it reveals an interesting analogy between the variable free surface area of the blob and the variable number of particles in a thermodynamical system with permeable boundaries. The equations determining the "exact" equilibrium state are mathematically well-posed but intractible because the invariants of motion depend nonquadratically on the phase coordinates. Progress unfortunately requires strong (but physically motivated) assumptions about the nature of the equilibrium state. Section 5 describes the numerical experiments.

2. Dynamical background

Consider first a single nonrotating layer of homogeneous fluid in which the horizontal length scales of the flow are large compared to the fluid depth. Then the horizontal velocity $\mathbf{u} = (u, v)$ in the (east, north) direction is invariant with depth and is much larger than the vertical velocity. The fluid motion is columnar. Let the positions $\mathbf{x} = (x, y)$ of marked fluid columns be considered as functions of curvilinear labeling coordinates (a, b), which remain constant following particles, and the time τ. The flow itself is a time-dependent map,

$$\begin{cases} x = x(a, b, \tau) \\ y = y(a, b, \tau) \end{cases} \tag{2.1}$$

from the (a, b) coordinates to the (x, y) coordinates. Each forward map of type (2.1) uniquely determines an inverse map

$$\begin{cases} a = a(x, y, t) \\ b = b(x, y, t) \end{cases} \tag{2.2}$$

from the (x, y) coordinates to the (a, b) coordinates. Here $t = \tau$, but $\partial/\partial\tau$ implies that (a, b) are held constant while $\partial/\partial t$ implies constant (x, y). It is convenient to define (a, b) so that equal areas in (a, b) space contain equal masses, that is,

$$h dx dy = da db, \tag{2.3}$$

where

$$h = \frac{\partial(a, b)}{\partial(x, y)} \tag{2.4}$$

is the depth of the fluid. Then the kinetic energy (omitting the contribution of vertical velocity) is

$$\begin{aligned} T &= \int\int dx dy \, \tfrac{1}{2}\rho_0 h \mathbf{u}\cdot\mathbf{u} \\ &= \tfrac{1}{2}\rho_0 \int\int da db \left[\left(\frac{\partial x}{\partial \tau}\right)^2 + \left(\frac{\partial y}{\partial \tau}\right)^2\right], \end{aligned} \tag{2.5}$$

where the integration extends over the domain of the fluid and ρ_0 is the constant fluid density. The potential energy is

$$\begin{aligned} V &= \int\int dx dy \, \tfrac{1}{2}\rho_0 g h^2 \\ &= \tfrac{1}{2}\rho_0 \int\int da db \left[g \frac{\partial(a, b)}{\partial(x, y)}\right], \end{aligned} \tag{2.6}$$

and the Lagrangian of the fluid is therefore

$$\begin{aligned} L &= T - V \\ &= \tfrac{1}{2}\rho_0 \int\int da db \left[\left(\frac{\partial x}{\partial \tau}\right)^2 + \left(\frac{\partial y}{\partial \tau}\right)^2 - g \frac{\partial(a, b)}{\partial(x, y)}\right]. \end{aligned} \tag{2.7}$$

It follows directly from the definition (2.4) that

$$\frac{\partial h}{\partial \tau} + h\left(\frac{\partial u}{\partial x} + \frac{\partial v}{\partial y}\right) = 0, \tag{2.8}$$

which is the usual equation of mass conservation. The momentum equations come from Hamilton's principle, which states that

$$\delta \int L d\tau = 0, \tag{2.9}$$

where δ denotes an arbitrary variation of the time-dependent map (2.1) or, equivalently, (2.2). If $\delta x(a, b, \tau)$, $\delta y(a, b, \tau)$ vanish for large $|a|$, $|b|$ and $|\tau|$, then, by the usual rules of variational calculus,

FIG. 2. The potential density sigma parameter referred to sea level, 2000 m and 4000 m in the (a) Atlantic, (b) Pacific and (c) Indian Oceans. These sections were drawn by Lynn and Reid (1968) from 25 years of hydrographic measurements.

δx:

$$\delta \int L d\tau = \rho_0 \int d\tau \iint dadb \times \left[\frac{\partial x}{\partial \tau}\frac{\partial}{\partial \tau}\delta x + \frac{gh^2}{2}\frac{\partial(\delta x, y)}{\partial(a, b)}\right] = \rho_0 \int d\tau \iint dadb\left[-\frac{\partial^2 x}{\partial \tau^2} - \frac{g}{2}\frac{\partial(h^2, y)}{\partial(a, b)}\right]\delta x \quad (2.10)$$

implies that

$$\frac{\partial^2 x}{\partial \tau^2} = -\frac{g}{2}\frac{\partial(h^2, y)}{\partial(a, b)} = -g\frac{\partial(h, y)}{\partial(x, y)}, \quad (2.11)$$

which is equivalent to the more familiar form,

$$\frac{\partial u}{\partial \tau} = -g\frac{\partial h}{\partial x}. \quad (2.12)$$

Similarly, of course,

δy:

$$\frac{\partial v}{\partial \tau} = -g\frac{\partial h}{\partial y}. \quad (2.13)$$

The Lagrangian formalism extends easily to include rotating coordinate systems and stratified flows. The Lagrangian for a single layer of uniformly rotating fluid is

$$L = \tfrac{1}{2}\rho_0 \iint dadb\left[\left(\frac{\partial x}{\partial \tau}\right)^2 + \left(\frac{\partial y}{\partial \tau}\right)^2 + 2\Omega\left(\frac{\partial y}{\partial \tau}x - \frac{\partial x}{\partial \tau}y\right) - g\frac{\partial(a, b)}{\partial(x, y)}\right], \quad (2.14)$$

or less symmetrically,

$$L = \tfrac{1}{2}\rho_0 \iint dadb\left[\left(\frac{\partial x}{\partial \tau}\right)^2 + \left(\frac{\partial y}{\partial \tau}\right)^2 - 4\frac{\partial x}{\partial \tau}\Omega y - g\frac{\partial(a, b)}{\partial(x, y)}\right], \quad (2.15)$$

where Ω is the rotation rate of the coordinate system. If Ω is nonconstant, but varies only in the y-coordinate direction, then the appropriate Lagrangian is

$$L = \tfrac{1}{2}\rho_0 \iint dadb\left[\left(\frac{\partial x}{\partial \tau}\right)^2 + \left(\frac{\partial y}{\partial \tau}\right)^2 - 4\frac{\partial x}{\partial \tau}\int_{y_0}^{y(a,b,\tau)} \Omega(y')dy' - g\frac{\partial(a, b)}{\partial(x, y)}\right], \quad (2.16)$$

where y_0 is arbitrary. The Lagrangian for the two-layer system introduced in section 1 turns out to be (with $2\Omega = \beta y$)

$$L = \rho_1 \iint da_1 db_1 \mathcal{L}_1 + \rho_2 \iint da_2 db_2 \mathcal{L}_2 + \rho_1 \iint da_1 db_1 \iint da_2 db_2 \mathcal{L}_{12}, \quad (2.17)$$

where

$$\mathcal{L}_i = \frac{1}{2}\left(\frac{\partial x_i}{\partial \tau}\right)^2 + \frac{1}{2}\left(\frac{\partial y_i}{\partial \tau}\right)^2 - \frac{\partial x_i}{\partial \tau}\int_{y_0}^{y_i} \beta y' dy' - \frac{g}{2}\frac{\partial(a_i, b_i)}{\partial(x_i, y_i)}, \quad (2.18)$$

$$\mathcal{L}_{12} = -g\delta(\mathbf{x}_1 - \mathbf{x}_2), \quad (2.19)$$

where the subscripts refer to the top ($i = 1$) and bottom ($i = 2$) layer, and $\delta(\ )$ is Dirac's delta function. Independent variations $\delta\mathbf{x}_1$, $\delta\mathbf{x}_2$ yield

$\delta\mathbf{x}_1$:

$$\frac{\partial \mathbf{u}_1}{\partial \tau} + \beta y_1 \mathbf{k} \times \mathbf{u}_1 = -g\nabla(h_1 + h_2), \quad (2.20)$$

$\delta\mathbf{x}_2$:

$$\frac{\partial \mathbf{u}_2}{\partial \tau} + \beta y_2 \mathbf{k} \times \mathbf{u}_2 = \frac{-g\rho_1}{\rho_2}\nabla h_1 - g\nabla h_2, \quad (2.21)$$

where $\mathbf{k}$ is the vertical unit vector and

$$h_i = \frac{\partial(a_i, b_i)}{\partial(x_i, y_i)} \quad (2.22)$$

is the vertical thickness of the i-th layer.

In all cases, an important *conservation law* called Ertel's theorem results from the *symmetry property* that the Lagrangian is unchanged by any transformation of the labeling coordinates (a, b) which leaves the Jacobians (2.4), and (2.22) unchanged. Consider, for example, the Langrangian (2.7) for the nonrotating single layer, and let $\delta a(x, y, t)$, $\delta b(x, y, t)$ be variations in the labeling coordinates which satisfy

$$\delta\frac{\partial(a, b)}{\partial(x, y)} = 0. \quad (2.23)$$

This implies that

$$\frac{\partial}{\partial a}\delta a + \frac{\partial}{\partial b}\delta b = 0, \quad (2.24)$$

and hence

$$\delta a = -\frac{\partial}{\partial b}\delta\psi \quad \text{and} \quad \delta b = \frac{\partial}{\partial a}\delta\psi \quad (2.25)$$

for some $\delta\psi$. For such a variation,

$$\delta \int L d\tau = \tfrac{1}{2}\rho_0 \int d\tau \iint dadb\,\delta\left[\left(\frac{\partial x}{\partial \tau}\right)^2 + \left(\frac{\partial y}{\partial \tau}\right)^2\right] = -\rho_0 \int d\tau \iint dadb\left[\left(\frac{\partial x}{\partial \tau}\frac{\partial x}{\partial a} + \frac{\partial y}{\partial \tau}\frac{\partial y}{\partial a}\right)\frac{\partial \delta a}{\partial \tau} + \left(\frac{\partial x}{\partial \tau}\frac{\partial x}{\partial b} + \frac{\partial y}{\partial \tau}\frac{\partial y}{\partial b}\right)\frac{\partial \delta b}{\partial \tau}\right], \quad (2.26)$$

since it can easily be shown that

$$\delta\left(\frac{\partial x}{\partial \tau}\right) = -\frac{\partial x}{\partial a}\frac{\partial \delta a}{\partial \tau} - \frac{\partial x}{\partial b}\frac{\partial \delta b}{\partial \tau}, \quad (2.27)$$

and similarly for $\delta(\partial y/\partial\tau)$. Substitution from (2.25) and integrations by parts bring (2.26) into the final form

$$\delta\int L d\tau = -\rho_0\int d\tau\iint dadb\left[\frac{\partial}{\partial\tau}\left(\frac{\partial B}{\partial a}-\frac{\partial A}{\partial b}\right)\right]\delta\psi, \tag{2.28}$$

where

$$A = \frac{\partial x}{\partial\tau}\frac{\partial x}{\partial a}+\frac{\partial y}{\partial\tau}\frac{\partial y}{\partial a}, \tag{2.29}$$

$$B = \frac{\partial x}{\partial\tau}\frac{\partial x}{\partial b}+\frac{\partial y}{\partial\tau}\frac{\partial y}{\partial b}. \tag{2.30}$$

But $\delta\psi$ is arbitrary and $\delta\int L d\tau$ must vanish by Hamilton's principle. Hence

$$\frac{\partial}{\partial\tau}\left(\frac{\partial B}{\partial a}-\frac{\partial A}{\partial b}\right) = 0. \tag{2.31}$$

The quantity in parentheses, which is conserved following particles, can be rewritten in a more familiar form as

$$\frac{\partial B}{\partial a}-\frac{\partial A}{\partial b} = \frac{\partial(u,x)}{\partial(a,b)}+\frac{\partial(v,y)}{\partial(a,b)} = \frac{\partial(x,y)}{\partial(a,b)} \times\left[\frac{\partial(u,x)}{\partial(x,y)}+\frac{\partial(v,y)}{\partial(x,y)}\right] = \left(\frac{\partial v}{\partial x}-\frac{\partial u}{\partial y}\right)h^{-1}. \tag{2.32}$$

The last expression is the usual form for the potential vorticity. Completely analogous procedures applied to the Lagrangians (2.15) and (2.17) lead to the respective forms of Ertel's theorem

$$\frac{\partial}{\partial\tau}\left[\left(\frac{\partial v}{\partial x}-\frac{\partial u}{\partial y}+\beta y\right)h^{-1}\right] = 0, \tag{2.33}$$

$$\frac{\partial}{\partial\tau_i}\left[\left(\frac{\partial v_i}{\partial x}-\frac{\partial u_i}{\partial y}+\beta y\right)h_i^{-1}\right] = 0, \quad i = 1, 2. \tag{2.34}$$

The foregoing procedure readily extends to continuously stratified, compressible flows (Ripa, 1981; Salmon, 1982). It provides an elegant unification for all forms of Ertel's theorem which is lacking in the conventional derivations: For *any* continuum system, Ertel's theorem is simply the conservation law which results from the most general transformation of labeling coordinates that leaves every term in the Lagrangian unchanged. This approach also provides a *motivation* for Ertel's theorem: The conservation law is known to exist as soon as an inspection of the Lagrangian reveals the symmetry property. One need not depend on unguided manipulations.[3]

[3] Eckart (1960) derived the conservation law (2.31) using the energy-momentum tensor formalism, which is closely related to the procedure followed here, but he did not notice the connection with Ertel's theorem. See also Bretherton (1970) for a closely related result.

3. Statistical mechanical background

The methods of equilibrium statistical mechanics predict the final macroscopic states toward which finite-resolution classical fluid models would evolve in the absence of external forcing and viscosity. These ideal equilibrium states anticipate the role of fluid self-interactions in realistic nonconservative flow. The pioneering papers were written by Onsager (1949), Hopf (1952) and Lee (1952). The equilibrium theory has frequently been used in the study of homogeneous turbulence, where it provides an important consistency check on non-equilibrium (closure) theories. However, the equilibrium theory seems most valuable when applied to even more complicated systems. For the more complicated systems, the closure theories are often prohibitively complex.

This section reviews the fundamental algorithm of equilibrium statistical mechanics from the information theory viewpoint (Jaynes, 1957). I illustrate the general method by application to ordinary two-dimensional turbulence. The equilibrium statistical mechanics of two-dimensional turbulence has been thoroughly discussed by Kraichnan and Montgomery (1980). Previous applications to geophysical fluid dynamics are reviewed by Salmon (1982). These include the locking of rotating flow to bottom topography, the barotropization of stratified rotating flow on length scales larger than the internal deformation radius, and the funneling of energy toward the equator and into high vertical modes.

Consider first a general mechanical system whose precise state is specified by the value of N real numbers $[\omega_1, \omega_2, \ldots, \omega_N]$ and whose dynamics is governed by N first-order ordinary differential equations of the form

$$\dot\omega_i \equiv \frac{d}{dt}\omega_i = G_i(\omega_1, \omega_2, \ldots, \omega_N). \tag{3.1}$$

The N-dimensional space spanned by the ω_i is called phase space, and each point in phase represents a possible state of the system as a whole. Every realization of (3.1) traces out a trajectory in phase space. Let the joint probability density of the ω_i in an ensemble of realizations of (3.1) be

$$\hat f(\omega_1, \omega_2, \ldots, \omega_N, t). \tag{3.2}$$

Since the moving phase points that represent individual realizations of (3.1) can neither be created nor destroyed,

$$\frac{\partial\hat f}{\partial t}+\sum_i\frac{\partial}{\partial\omega_i}(\dot\omega_i\hat f) = 0, \tag{3.3}$$

where $\dot\omega_i$ is given by (3.1). If (3.1) is such that

$$\sum_i\frac{\partial\dot\omega_i}{\partial\omega_i} = 0, \tag{3.4}$$

then (3.3) reduces to

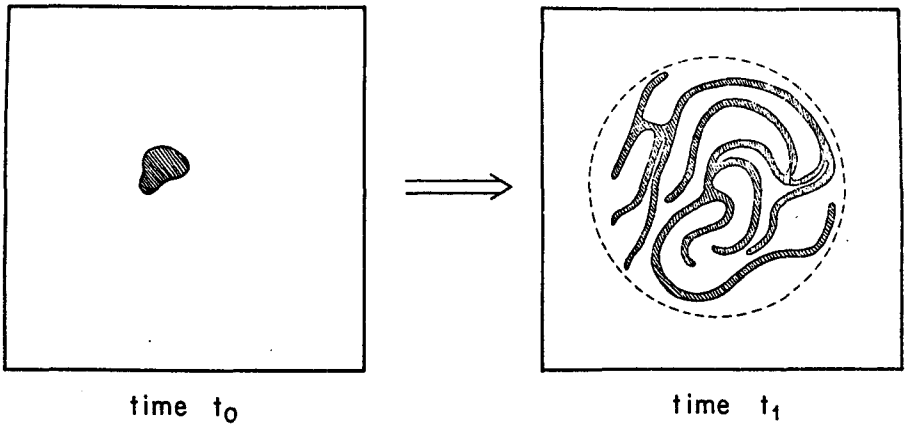

FIG. 3. The mixing of probability density in a two-dimensional phase space.

$$\frac{\partial \hat{f}}{\partial t} + \sum_i \dot{\omega}_i \frac{\partial \hat{f}}{\partial \omega_i} = 0, \tag{3.5}$$

which is called Liouville's theorem. Canonical variables satisfy (3.4) automatically, but so too do many noncanonical variables, and the latter are frequently of greater interest.

Eq. (3.5) implies that the phase space volume occupied by a collection of phase particles always containing the same particles remains constant in time. This constraint, while important, is not confining. Consider, for example, a two-dimensional phase space in which $\hat{f}$ is initially constant within a compact region and zero outside (Fig. 3). In a wide class of systems, which are said to "mix," the initially compact region spreads out by developing filamentous arms which gradually "fill up" the accessible parts of phase space. Now $\hat{f}$ is typically sought for computing the statistical average of phase functions $F(\omega_1, \omega_2, \ldots, \omega_N, t)$, namely

$$\langle F \rangle = \iiint \cdots \int F\hat{f}(\prod_i d\omega_i). \tag{3.6}$$

Suppose that $\hat{f}$ does indeed evolve from time t_0 to t_1 as shown in Fig. 3. In practice, it is impossible to calculate $\hat{f}(t_1)$ accurately from (3.5) for use in (3.6). However, it is obvious that, for any F which depends smoothly on its arguments, $\langle F \rangle$ at t_1 can be calculated to good accuracy by replacing $\hat{f}(t_1)$ with a density function which is constant over the circular region of Fig. 3. We therefore distinguish between $\hat{f}(t)$, the probability density obtained from (3.5) by solution of (3.1) for an entire ensemble of systems, and $f(t)$, the "phenomenological" or practical density, which can be considered a smoothed version of $\hat{f}(t)$. Statistical mechanics seeks $f(t)$ without first calculating $\hat{f}(t)$. The mixing property of the dynamics motivates the concept of $f(t)$, but it also imposes the consistency requirement that $f(t)$ ought to be progressively more spread out at successively later times. This is a qualitative statement of the second law of thermodynamics.

The entropy S measures the spread of f and the corresponding uncertainty in precise system state. A simple requirement on additivity, and the Liouville property (3.4), motivate the definition[4]

$$S = -\iiint \cdots \int f \ln f(\prod_i d\omega_i). \tag{3.7}$$

Now suppose that, at some fixed time t_0, it is known *only* that M dynamical quantities R_j take the average values R_j^0. The least-biased estimate for $f(t_0)$ is that which maximizes (3.7) subject to the M constraints

$$\iiint \cdots \int R_j f(\prod_i d\omega_i) = R_j^0,$$

$$j = 1, \ldots, M. \tag{3.8}$$

With f so determined, the least-biased estimate of $\langle F \rangle$ at time t_0 is just

$$\iiint \cdots \int Ff(\prod_i d\omega_i), \tag{3.9}$$

where F is any quantity, whatsoever. If the set $\{R_j\}$ includes only integral constants of motion, then f describes *absolute equilibrium*, which is pertinent at times so large that all vestiges of the initial conditions, except constants of the motion, have disappeared. Realistic dissipative systems have no conserved quantities and cannot therefore reach this type of equilibrium. However, if the "mixing time" is short compared to the time for nonconservative forcing to alter the values of these quantities, then qualitative features of absolute equilibrium can appear in realistic systems.

I illustrate the general procedure by application to

[4] See, for example, Katz (1967).

inviscid incompressible two-dimensional flow within closed boundaries, governed by

$$\frac{\partial \mathbf{u}}{\partial \tau} = -\nabla p, \quad \nabla \cdot \mathbf{u} = 0, \tag{3.10}$$

or, equivalently, by

$$\frac{\partial}{\partial \tau}(\nabla^2 \psi) = 0, \tag{3.11}$$

where

$$\mathbf{u} = \mathbf{k} \times \nabla \psi \quad \text{and} \quad \nabla = \left(\frac{\partial}{\partial x}, \frac{\partial}{\partial y}\right).$$

It is convenient to expand

$$\psi(x, y, t) = \sum_i \omega_i(t)\varphi_i(x, y)/k_i, \tag{3.12}$$

where $\varphi_i(\mathbf{x})$ is a normalized eigenfunction satisfying

$$\begin{cases} \nabla^2 \varphi_i + k_i^2 \varphi_i = 0 \\ \varphi_i = 0 \text{ on the boundary} \\ \overline{\varphi_i^2} = 1. \end{cases} \tag{3.13}$$

Here the overbar denotes the spatial average over the flow domain. The transform of (3.11) is

$$\dot{\omega}_i = \sum_{j,l} A_{ijl}\omega_j\omega_l, \tag{3.14}$$

where

$$A_{ijl} = (k_j/k_i k_l)\overline{\varphi_i J(\varphi_l, \varphi_j)}. \tag{3.15}$$

Eqs. (3.4) and (3.5) are satisfied because A_{ijl} vanishes whenever two of its subscripts are equal. The constants of the motion include the energy

$$E = \overline{\nabla\psi\nabla\psi} = \sum_i \omega_i^2 \overset{\text{def}}{=} \sum_i E_i \tag{3.16}$$

and enstrophy

$$Z = \overline{(\nabla^2\psi)^2} = \sum_i k_i^2\omega_i^2 \overset{\text{def}}{=} \sum_i Z_i. \tag{3.17}$$

Absolute equilibrium is discovered by maximizing (3.7) subject to the normalization requirement

$$\langle 1 \rangle = 1 \tag{3.18}$$

and

$$\langle E \rangle = E_0, \quad \langle Z \rangle = Z_0, \tag{3.19}$$

where E_0 and Z_0 are known initial values. The result is

$$f = K \exp(-aE - bZ), \tag{3.20}$$

where a, b, K are multipliers determined from (3.18) and (3.19). From (3.20) it follows that

$$\langle \omega_i^2 \rangle = \tfrac{1}{2}(a + bk_i^2)^{-1}, \tag{3.21}$$

which shows that the quantity $aE_i + bZ_i$ is equi-partitioned among the modes in equilibrium.

Eq. (3.21) implies an energy spectrum proportional to

$$k/(a + bk^2), \tag{3.22}$$

which corresponds to infinite total energy and enstrophy, because the integrals of (3.22) diverge at large wavenumber k. The absolute equilibrium state is therefore realizable only if the sums in (3.14)–(3.17) are truncated to a finite number of terms, as if, for example, all modes with wavenumber k greater than some arbitrarily chosen cut-off k_c were excluded from the dynamics. The truncated system still satisfies (3.4). A thought experiment in which k_c is raised by finite increments, with the system allowed to re-equilibrate at each new value of k_c provides one "proof" that nonlinear interactions in two-dimensional turbulence pass energy to lower wavenumbers and enstrophy to higher wavenumbers (Kraichnan, 1975).[5] The equilibrium spectrum (3.22) has been verified in numerical experiments by many investigators, including Fox and Orszag (1973), Kells and Orszag (1978) and Carnevale (1982).

The objection can here be raised that the dynamics (3.11) actually conserve an infinite number of quantities of the form,

$$\overline{(\nabla^2\psi)^n},$$

where n is any number for which the average exists. These invariants constitute an infinite number of (generally nonquadratic) constraints which, along with (3.19), ought to determine the equilibrium state. These extra invariants are, however, usually neglected, because they lead to integrals which cannot be performed. The justification is sometimes given that, except for the case $n = 2$, the extra invariants do not survive the truncation in modes. Unfortunately, this argument does not so much strengthen the case for (3.20) as it weakens the case for realistic truncated models. I prefer the more pragmatic viewpoint that 1) statistical mechanics is merely an algorithm for guessing without bias, 2) not every known invariant need necessarily be used, and 3) the simplest invariants are frequently the most confining and hence important.

The eigenfunction expansion (3.12) can be avoided. Suppose that (3.11) is replaced directly by the truncated form

$$\frac{d}{dt}\psi_i = \sum_{j,l} B_{ijl}\psi_j\psi_l, \tag{3.23}$$

where ψ_i is the value of ψ at the ith gridpoint (x_i, y_i) and the right side of (3.23) is a difference approximation to

[5] It is of course unnecessary to invoke absolute equilibrium to explain the inverse energy transfer in two-dimensional flow. However, *some* form of averaging is required. Otherwise the time reversibility of (inviscid) mechanics provides a counter-example for every example.

$$-\frac{1}{\nabla^2} J(\psi, \nabla^2\psi) \tag{3.24}$$

within the given boundaries. The ψ_i comprise a new set of phase coordinates, and (3.4)–(3.5) hold with ω_i replaced by ψ_i. The truncated invariants become

$$E = -\overline{\psi\nabla^2\psi} \propto -\sum_i \sum_j \psi_i L_{ij} \psi_j \tag{3.25}$$

and

$$Z = \overline{(\nabla^2\psi)^2} \propto \sum_i (\sum_j L_{ij}\psi_j)^2, \tag{3.26}$$

where $\sum_j L_{ij}\psi_j$ is a difference approximation to $\nabla^2\psi$ at the ith gridpoint. The equilibrium probability density of the ψ_i is then

$$f(\psi_1, \psi_2, \ldots, \psi_N, t) = K' \exp[-\tfrac{1}{2} \sum_{i,j} \psi_i M_{ij} \psi_j], \tag{3.27}$$

where

$$M_{ij} = -2a' L_{ij} + 2b' \sum_l L_{li} L_{lj}, \tag{3.28}$$

and K', a', b' are determined from (3.18) and (3.19). It follows directly from (3.27) that

$$\langle \psi_i \psi_j \rangle = M_{ij}^{-1}, \tag{3.29}$$

where M^{-1} is the inverse of the matrix M. Thus

$$\sum_j M_{ij} \langle \psi_j \psi_k \rangle = \delta_{ik}, \tag{3.30}$$

which is the difference form of

$$(-2a'\nabla^2 + 2b'\nabla^2\nabla^2)\langle \psi(\mathbf{x})\psi(\mathbf{x}_0)\rangle = \delta(\mathbf{x} - \mathbf{x}_0), \tag{3.31}$$

corresponding to no truncation. The transform of (3.31) is

$$\langle \omega_i \omega_j \rangle = \tfrac{1}{2}(a + bk_i^2)^{-1}\delta_{ij}, \tag{3.32}$$

which agrees with (3.21).

It is sometimes useful to apply the statistical mechanics algorithm in two stages, assuming first a detailed knowledge of the distribution of energy and other invariants among the components. Section 4 illustrates the advantages of this procedure, but the idea is better introduced here, in the simpler context. Suppose that the statistical information consists not of (3.19), but rather

$$\langle \omega_i \omega_j \rangle = C_{ij}, \quad \text{all } i \text{ and } j, \tag{3.33}$$

where C_{ij} are known constants at the given time. The probability density f which maximizes S subject to (3.18) and (3.33) is just

$$f = K \exp(-\sum_{i,j} a_{ij}\omega_i\omega_j), \tag{3.34}$$

where K, a_{ij} are chosen to satisfy (3.18) and (3.33). These requirements establish that

$$K = (2\pi)^{-N/2}(\det C)^{-1/2}, \tag{3.35}$$

$$a_{ij}^{-1} = 2C_{ij}, \tag{3.36}$$

so that (3.34) may be rewritten

$$f = \frac{1}{(\sqrt{2\pi})^N} \frac{1}{\sqrt{\det\langle \omega_i\omega_j\rangle}} \tag{3.37}$$

$$\times \exp[-\tfrac{1}{2} \sum_{i,j} \omega_i \langle \omega_i\omega_j\rangle^{-1}\omega_j], \tag{3.37}$$

where $\langle \omega_i\omega_j\rangle^{-1}$ is the inverse of the known correlation matrix $\langle \omega_i\omega_j\rangle$. The entropy corresponding to (3.37) is

$$S = -\int\int\int \cdots \int f \ln f (\prod_i d\omega_i)$$

$$= \tfrac{1}{2} \ln(\det\langle \omega_i\omega_j\rangle) + \text{constant}. \tag{3.38}$$

If the correlation matrix is diagonal (as in statistically homogeneous flow) then the entropy simplifies to

$$S = \tfrac{1}{2} \sum_i \ln\langle \omega_i^2 \rangle. \tag{3.39}$$

The result (3.21) can now be obtained simply by maximizing (3.39) subject to

$$\sum_i \langle \omega_i^2 \rangle = E_0, \tag{3.40}$$

$$\sum_i k_i^2 \langle \omega_i^2 \rangle = Z_0. \tag{3.41}$$

This procedure works equally well if (3.40)–(3.41) are replaced by any constraints involving only second moments of the ω_i. But if (for example) constraints involving the first moments $\langle \omega_i \rangle$ need also be considered, then the $\langle \omega_i \rangle$ must be added to the list (3.33) of initial information.

The two-stage procedure has two advantages. First, formulas like (3.39) frequently admit useful interpretations. For example, a well-known class of turbulence theories provides closed time-evolution equations for the second moments $\langle \omega_i\omega_j\rangle$. Carnevale *et al.* (1981) have shown that these equations are consistent with

$$\frac{dS}{dt} \geq 0, \tag{3.42}$$

with S given by (3.38). Second, there sometimes exist important but nonquadratic constraints which must be replaced by approximations involving integrable moments. Then the two-stage procedure greatly simplifies the arithmetic. The following section is a good illustration.

4. Statistical mechanics of the blob

For the remainder of this paper, I restrict attention to the two-layer rotating system governed by (2.20) and (2.21), with an additional assumption that the lower layer velocity is everywhere small compared to that within the blob. This assumption is valid if, for

example, the initial excitation is confined to the blob and the lower layer is infinitely deep. A vanishing lower layer velocity implies from (2.21) that

$$\nabla h_2 = -\frac{\rho_1}{\rho_2}\nabla h_1, \tag{4.1}$$

so that the dynamics reduce to

$$\left.\begin{aligned} \frac{\partial u}{\partial \tau} - \beta y v &= -g'\frac{\partial h}{\partial x} \\ \frac{\partial v}{\partial \tau} + \beta y u &= -g'\frac{\partial h}{\partial y} \\ \frac{\partial h}{\partial \tau} + h\left(\frac{\partial u}{\partial x} + \frac{\partial v}{\partial y}\right) &= 0 \end{aligned}\right\}, \tag{4.2}$$

where $g' \equiv (\rho_2 - \rho_1)g/\rho_2$ and (u, v) and h are the horizontal velocity and vertical thickness of the blob. The equations (4.2a, b) are equivalent to

$$\frac{\delta}{\delta x}, \frac{\delta}{\delta y}\int L d\tau = 0, \tag{4.3}$$

where

$$L = \tfrac{1}{2}\rho_0 \iint dadb\left[\left(\frac{\partial x}{\partial \tau}\right)^2 + \left(\frac{\partial y}{\partial \tau}\right)^2 - \beta y^2\frac{\partial x}{\partial \tau} - g'\frac{\partial(a, b)}{\partial(x, y)}\right], \tag{4.4}$$

$$h = \frac{\partial(a, b)}{\partial(x, y)}. \tag{4.5}$$

The Lagrangian (4.4) differs from the "barotropic" Lagrangian (2.16) only in that the gravity g is replaced by the reduced gravity g'. For this reason, (4.2) is sometimes called the "equivalent barotropic model". I offer that the basic results obtained below will extend qualitatively to the unconstrained two-layer model. A sequel paper will entertain an N-layer ocean.

In order to apply the methods of Section 3 to the model (4.2), it is first necessary to discover a truncated dynamics which satisfies Liouville's theorem. Suppose temporarily that the blob covers the lower layer in the entire domain of interest, a region R_{xy} of the (x, y) plane bounded by rigid vertical walls. Let R_{xy} be subdivided into N square grids of side Δ. The ith gridbox is that centered on (x_j, y_k) where $i \leftrightarrow (j, k)$ is an integer index which runs from 1 to N. It is convenient to have

$$x_{j+1} = x_j + \Delta \quad \text{and} \quad y_{k+1} = y_k + \Delta.$$

Replace (4.2) by the difference equations

$$\left.\begin{aligned} \dot{U}_i &= \beta y_k V_i - (A_{j+1,k} - A_{j-1,k})/2\Delta \\ \dot{V}_i &= -\beta y_k U_i - (B_{j,k+1} - B_{j,k-1})/2\Delta \\ \dot{h}_i &= -(C_{j+1,k} - C_{j-1,k})/2\Delta \\ &\quad - (D_{j,k+1} - D_{j,k-1})/2\Delta \end{aligned}\right\}, \tag{4.6}$$

where

$$U_i = u(x_j, y_k)h(x_j, y_k),$$
$$V_i = v(x_j, y_k)h(x_j, y_k),$$
$$h_i = h(x_j, y_k),$$

and

$$A_{j,k} = U_i^2/h_i + U_iV_i/h_i + gh_i^2/2,$$
$$B_{j,k} = V_i^2/h_i + U_iV_i/h_i + gh_i^2/2,$$
$$C_{j,k} = U_i$$
$$D_{j,k} = V_i.$$

It follows at once that

$$\frac{\partial \dot{U}_i}{\partial U_i} = \frac{\partial \dot{V}_i}{\partial V_i} = \frac{\partial \dot{h}_i}{\partial h_i} = 0, \tag{4.7}$$

so that the $3N$-dimensional phase space spanned by $\{U_1, V_1, h_1, \ldots, U_N, V_N, h_N\}$ satisfies Liouville's theorem. The probability density function

$$f(U_1, V_1, h_1, \ldots, U_N, V_N, h_N) \tag{4.8}$$

may now be introduced and manipulated as in Section 3.

Suppose next that the blob covers only a subset of the N gridboxes in R_{xy}. Each possible subset of gridboxes, which need not be contiguous in the (x, y) plane, will be called a *configuration* of the system (Fig. 4). The number of possible different configurations is

$$\sum_{n=1}^{N}\frac{N!}{n!(N-n)!}. \tag{4.9}$$

Let γ be an integer index that specifies the configuration, and N_γ be the number of gridboxes in configuration γ. The precise system state is specified by a value for γ and by the location of a point in the corresponding $3N_\gamma$-dimensional phase space. Let f_γ be the probability density function in this γ-space and let

$$T_\gamma(\ ) \overset{\text{def}}{=} \iiint \cdots \int (\ )\prod_{i=1}^{N_\gamma}(dU_i dV_i dh_i) \tag{4.10}$$

denote an integration over the entire γ-space. Then

$$P_\gamma \overset{\text{def}}{=} T_\gamma(f_\gamma) \tag{4.11}$$

is just the probability that the system finds itself in configuration γ. The normalization requirement

$$\sum_\gamma P_\gamma = 1 \tag{4.12}$$

obtains because the system is always in precisely one configuration. Now let F_γ be any function that depends only on the $3N_\gamma$ phase coordinates of configuration γ. The average of F_γ, conditional on configuration γ, is by definition

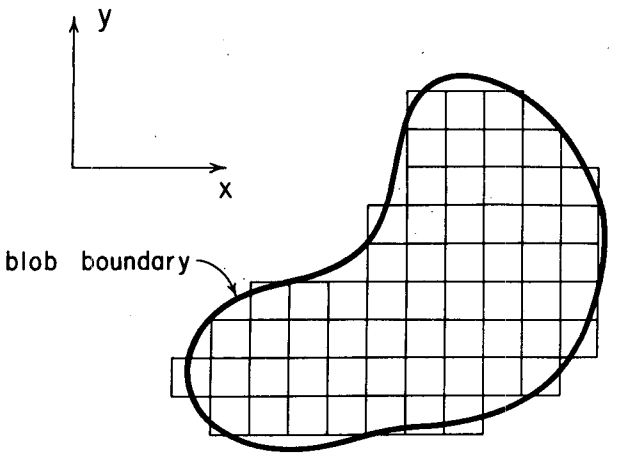

FIG. 4. The surface of the blob covers a subset of gridboxes.

$$\langle F_\gamma \rangle_\gamma \overset{\text{def}}{=} T_\gamma(F_\gamma f_\gamma)/P_\gamma. \tag{4.13}$$

For example, the average total volume, given the blob in configuration γ, is $\langle M_\gamma \rangle_\gamma$, where

$$M_\gamma = \Delta^2 \sum_{i\in\gamma} h_i, \tag{4.14}$$

and the sum runs only over gridboxes in the configuration γ. The "grand average" total volume is

$$\langle M \rangle \overset{\text{def}}{=} \sum_\gamma P_\gamma \langle M_\gamma \rangle_\gamma = \sum_\gamma T_\gamma(M_\gamma f_\gamma), \tag{4.15}$$

where M, strictly speaking, is a sequence of phase functions $\{M_\gamma\}$ defined by (4.14). Note that this definition of the angle braces gives a finite value to

$$\left\langle \frac{1}{h_i} \right\rangle, \tag{4.16}$$

the grand average of $1/h$ at the ith gridbox. Absolute equilibrium is discovered by maximizing the appropriate entropy (derived below) subject to the normalization requirement (4.12) and constraints on the invariants of motion, expressed as grand averages. The integral invariants of the system (4.2) include the total mass, total energy, and every quantity of the form

$$\iint dxdyhF(q), \tag{4.17}$$

where

$$q = \left(\frac{\partial v}{\partial x} - \frac{\partial u}{\partial y} + \beta y\right) h^{-1} \tag{4.18}$$

is the potential vorticity and F is any function for which the integral (4.17) exists at the initial time. The total potential vorticity and potential enstrophy are cases of (4.17), corresponding to $F = q$ and $F = q^2$, respectively.

It is now convenient to restrict the phase space averages to be averages on the *geostrophic manifold*, which is defined by difference analogs to the geostrophic relations, for example

$$U_i = -\frac{g'}{2\beta y_i}[h^2(x_j, y_k + \Delta) - h^2(x_j, y_k - \Delta)]/2\Delta. \tag{4.19}$$

Eq. (4.19) and its counterpart for V_i are used to eliminate U_i and V_i from every expression in which they occur, and the definition (4.10) is replaced by

$$T_\gamma(\ ) \overset{\text{def}}{=} \int_0^\infty \int_0^\infty \int_0^\infty \cdots \int_0^\infty (\ ) \prod_{i=1}^{N_\gamma} dh_i. \tag{4.20}$$

The geostrophic average can be interpreted as the average over the low-frequency part of the flow. The total mass, energy, potential vorticity and potential enstrophy are now written in terms of the depth variables only, as

$$\left.\begin{aligned} M_\gamma &= \sum_{i\in\gamma} h_i \\ E_\gamma &= \sum_{i\in\gamma} h_i[(\sum_{j\in\gamma} X_{ij}h_j)^2 + (\sum_{j\in\gamma} Y_{ij}h_j)^2 + g'h_i] \\ V_\gamma &= \sum_{i\in\gamma} (\sum_{j\in\gamma} L_{ij}h_j + \beta y_i) \\ Z_\gamma &= \sum_{i\in\gamma} (\sum_{j\in\gamma} L_{ij}h_j + \beta y_i)^2/h_i \end{aligned}\right\}, \tag{4.21}$$

where X_{ij}, Y_{ij} and L_{ij} are difference forms for the differential operators

$$\frac{g'}{\beta y}\frac{\partial}{\partial x}, \quad \frac{g'}{\beta y}\frac{\partial}{\partial y} \quad \text{and} \quad \nabla\cdot\left(\frac{g'}{\beta y}\nabla\right),$$

respectively.[6] The invariant constraints then take the form,

$$\left.\begin{aligned} \langle M \rangle &= \mathrm{M}_0, \quad \langle E \rangle = E_0 \\ \langle V \rangle &= \mathrm{V}_0, \quad \langle Z \rangle = Z_0 \end{aligned}\right\}, \tag{4.22}$$

where M_0, E_0, V_0, Z_0 are the known initial values. A more detailed (and correct) statement would replace the angle braces in (4.22) with $\langle\ \rangle_\gamma$, thereby demanding that the mass, energy, etc., be the same in each separate configuration. However, this alternative requires more calculation, and the change in the results should be slight, if, as is usually the case, the probability P_γ of configurations is sharply peaked at the most probable γ. If, as is henceforth assumed, the statistics have cross-equatorial symmetry between the hemispheres, then $V_0 = 0$ and $\langle V \rangle = 0$ automatically. The third of (4.22) can therefore be dropped.

[6] Again one can inquire whether the truncated dynamics actually conserve (4.21), and, if not, whether suitable replacements could be found. In the information theory viewpoint, however, consistency demands only that the invariants remain constant over times long enough for the system to sample many independent states.

Unfortunately, direct use of (4.22) demands integrals like

$$\int_0^\infty \int_0^\infty \cdots \int_0^\infty \exp(-\text{constant} \times E_\gamma) \prod_i dh_i, \tag{4.23}$$

which cannot be performed. My recourse is to replace (4.22) with the approximate constraints

$$\left.\begin{aligned} &\sum_\gamma P_\gamma \sum_{i\in\gamma} \langle h_i\rangle_\gamma = M_0, \\ &\sum_\gamma P_\gamma E_i^\gamma \overset{\text{def}}{=} \sum_\gamma P_\gamma \sum_{i\in\gamma} \langle h_i\rangle_\gamma [(\sum_{j\in\gamma} X_{ij}\langle h_j\rangle_\gamma)^2 \\ &\qquad + (\sum_{j\in\gamma} Y_{ij}\langle h_j\rangle_\gamma)^2 + g'\langle h_i\rangle_\gamma] = E_0 \\ &\sum_\gamma P_\gamma Z_i^\gamma \overset{\text{def}}{=} \sum_\gamma P_\gamma \sum_{i\in\gamma} \\ &\qquad \times [\sum_{j\in\gamma} L_{ij}\langle h_j\rangle_\gamma + \beta y_i]^2/\langle h_i\rangle_\gamma = Z_0 \end{aligned}\right\}, \tag{4.24}$$

in which, unlike (4.22), only first moments of the depth appear. This approximation is justified if, at the large length and time scales considered, the fluctuations in thermocline depth are small compared to $\langle h\rangle_\gamma$, in each configuration γ.

Now suppose that each γ-space is divided into hypercubes of side d and volume d^{N_γ}. The probability that the system is in a configuration γ *and* a particular hypercube in the corresponding γ-space is by definition

$$p_j = f_\gamma d^{N_\gamma}, \tag{4.25}$$

where f_γ is evaluated at the cube, and

$$j \leftrightarrow (\gamma, \text{cube})$$

is an index which denotes both the space and cube. The total entropy is

$$\begin{aligned} S &= -\sum_j p_j \ln p_j \\ &= -\sum_{\gamma\ \text{cubes}} \sum (f_\gamma d^{N_\gamma}) \ln(f_\gamma d^{N_\gamma}) \\ &= -\sum_{\gamma\ \text{cubes}} \sum (f_\gamma \ln f_\gamma)(d^{N_\gamma}) \\ &\qquad - \sum_{\gamma\ \text{cubes}} \sum (f_\gamma N_\gamma \ln d)(d^{N_\gamma}). \end{aligned} \tag{4.26}$$

In the limit $d \to 0$,

$$S \to -\sum_\gamma T_\gamma(f_\gamma \ln f_\gamma) - \sum_\gamma N_\gamma T_\gamma(f_\gamma) \ln d. \tag{4.27}$$

The entropy depends on the depth resolution d, which must be nonzero, and is entirely analogous to the horizontal resolution Δ. The choice of d affects equilibrium, because the second term in (4.27) also contains f_γ. This situation is quite unlike the example of Section 3 in which the resolution on each ψ_i was unlimited. It is interesting, however, that the present dependence of the equilibrium on d would *disappear* if the blob could assume only one configuration. To see this, suppose $P_{\gamma_0} = 1$ for some γ_0, and $P_\gamma = 0$ for all other γ. Then (4.27) reduces to

$$S = -T_{\gamma_0}(f_{\gamma_0} \ln f_{\gamma_0}) - N_\gamma \ln d, \tag{4.28}$$

because (4.12) becomes

$$T_{\gamma_0}(f_{\gamma_0}) = 1. \tag{4.29}$$

The second term of (4.28) has no variation with f_{γ_0}, and hence is irrelevant. However, this is *not* true for the second term in (4.27).

There exists an interesting but incomplete analogy between the fluid blob and a classical gas composed of an indefinite number of particles (the grand canonical ensemble). In the gas system, the dimensionality of phase space varies with the number of particles present, and the calculation follows the same line as here. However, no artificial parameter like d appears because the average number of particles is fixed as a constraint. There are of course no physical grounds for constraining the analogous surface area of the blob. Also, in the gas calculation the counterpart of (4.13) contains a factor $1/N_\gamma!$ to prevent the overcounting of states corresponding to the permutations of identical particles. This factor is absent from the blob calculation because the gridboxes are non-identical; each is distinguished by its horizontal location.

The remaining task is to obtain the equilibrium f_γ by maximizing the entropy (4.27) subject to the normalization requirement (4.12) and the constraints (4.24). As remarked in Section 3, this labor is best divided into two stages. First, Eq. (4.27) is maximized subject to the constraints

$$T_\gamma(f_\gamma) = P_\gamma, \quad \text{all } \gamma, \tag{4.30}$$

and

$$T_\gamma(h_i f_\gamma) = \langle h_i\rangle_\gamma P_\gamma, \quad \text{all } \gamma, \quad \text{all } i \in \gamma, \tag{4.31}$$

where the P_γ and $\langle h_i\rangle_\gamma$ are here treated as known constants. The result is

$$f_\gamma = C_\gamma d^{-N_\gamma} \exp[-\sum_{i\in\gamma} \lambda_i^\gamma h_i], \tag{4.32}$$

where the C_γ and λ_i^γ are determined from (4.30) and (4.31). After such determination,

$$f_\gamma = P_\gamma e^{-N_\gamma} \prod_{i\in\gamma} \left\{\frac{1}{\langle h_i\rangle_\gamma} \exp\left[-\frac{(h_i - \langle h_i\rangle_\gamma)}{\langle h_i\rangle_\gamma}\right]\right\}. \tag{4.33}$$

Substitution of (4.33) into (4.27) yields

$$\begin{aligned} S = &-\sum_\gamma P_\gamma \ln P_\gamma + \sum_\gamma P_\gamma N_\gamma \\ &+ \sum_\gamma P_\gamma \sum_{i\in\gamma} \ln\left(\frac{\langle h_i\rangle_\gamma}{d}\right). \end{aligned} \tag{4.34}$$

The *equilibrium* values for P_γ and $\langle h_i\rangle_\gamma$ may now be found by maximizing (4.34) subject to (4.24). The first two terms in (4.34) represent the entropy associated with the uncertainty in the configuration of the blob. The first term, if present alone, would make all configurations equally probable. The second term adds a bias favoring configurations with large surface area (large N_γ). The third term in (4.34) represents the entropy associated with the distribution of mass within each configuration. If only one fixed configuration were allowed, as if the blob always covered the bottom layer completely, then (4.34) would reduce to

$$S = \sum_i \ln\langle h_i\rangle + \text{irrelevant constants}, \quad (4.35)$$

which is similar to (3.39).

Now suppose, for illustration, that mass conservation (4.24a) is the only equilibrium constraint besides the normalization (4.12). Maximizing

$$S - \lambda[\sum_\gamma P_\gamma - 1] - a[\sum_\gamma P_\gamma \sum_{i\in\gamma} \langle h_i\rangle_\gamma - M_0] \quad (4.36)$$

yields

δP_γ:

$$-\ln P_\gamma - 1 + N_\gamma + \sum_{i\in\gamma} \ln\left(\frac{\langle h_i\rangle_\gamma}{d}\right) - \lambda - a\sum_{i\in\gamma}\langle h_i\rangle_\gamma = 0, \quad (4.37)$$

$\delta\langle h_i\rangle_\gamma$:

$$\frac{P_\gamma}{\langle h_i\rangle_\gamma} - aP_\gamma = 0, \quad (4.38)$$

for all γ and all $i \in \gamma$, where a and λ are the Lagrange multipliers. From (4.38) it follows that the thermocline depth

$$\langle h_i\rangle_\gamma = \frac{1}{a} \quad (4.39)$$

is the same in all configurations and at all locations, whereupon (4.37) simplifies to

$$P_\gamma = K\left(\frac{\langle h\rangle_\gamma}{d}\right)^{N_\gamma}. \quad (4.40)$$

The constants a and K are determined from (4.24a) and (4.12). Now since $\langle h\rangle_\gamma \geqslant d$, P_γ increases with N_γ, and the most probable configurations are those in which no more than one "fluid brick" of volume $d\Delta^2$ occupies each gridbox. Thus the equilibrium state with only mass conserved has the blob spread out to the minimum thickness that the vertical resolution will allow.

Consider next a more realistic case in which the recognized invariants of motion include the mass (4.24a) and an approximation to the potential enstrophy (4.24c) in the form

$$\sum_\gamma P_\gamma \sum_{i\in\gamma} \beta^2 y_i^2/\langle h_i\rangle_\gamma = Z_0. \quad (4.41)$$

The approximation (4.41) is reasonable if the relative vorticity is much smaller than the planetary vorticity βy. This condition is satisfied by the real ocean at all latitudes more than a few degrees from the equator. However, (4.41) is still suspect in the present context, because the equilibrium state, which is reached after friction has been turned off, could plausibly have large relative vorticity. Maximizing

$$S - \lambda[\sum_\gamma P_\gamma - 1] - a[\sum_\gamma P_\gamma \sum_{i\in\gamma}\langle h_i\rangle_\gamma - M_0] - b[\sum_\gamma P_\gamma \sum_{i\in\gamma} \beta^2 y_i^2/\langle h_i\rangle_\gamma - Z_0] \quad (4.42)$$

leads to

δP_γ:

$$P_\gamma = Ke^{N_\gamma}\prod_{i\in\gamma}\left\{\frac{\langle h_i\rangle_\gamma}{d}\exp[-a\sum_{i\in\gamma}\langle h_i\rangle_\gamma - b\sum_{i\in\gamma}\beta^2 y_i^2/\langle h_i\rangle_\gamma]\right\}, \quad (4.43)$$

$\delta\langle h_i\rangle_\gamma$:

$$1 = a\langle h_i\rangle_\gamma - b\beta^2 y_i^2/\langle h_i\rangle_\gamma, \quad (4.44)$$

where the constants K, a, b are determined from (4.12) (4.24a) and (4.41). Eq. (4.44) states that a weighted *difference* between the mass and potential enstrophy is equipartitioned among the gridboxes. Apply $\sum_{i\in\gamma}$ to (4.44) and use the result to simplify (4.43). Then (4.43) becomes

$$P_\gamma = K\prod_{i\in\gamma}\left[\frac{\langle h_i\rangle_\gamma}{d}\exp(-2b\sum_{i\in\gamma}\beta^2 y_i^2/\langle h_i\rangle_\gamma)\right]. \quad (4.45)$$

The previous case with only mass conserved is recovered when $b = 0$. The solution to (4.44) is

$$\langle h_i\rangle_\gamma = \frac{1}{2a}[1 + (1 + 4ab\beta^2 y_i^2)^{1/2}], \quad (4.46)$$

which depends only on the latitude y_i. Since this solution applies to all configurations γ, including those containing arbitrarily many of the gridboxes, and since $\langle h_i\rangle_\gamma > 0$ within each configuration, it follows that a, b must be positive and that only the positive branch of (4.46) has meaning. The simple quadratic (4.46) has a nearly constant depth,

$$\langle h\rangle_\gamma \approx \frac{1}{a} \overset{\text{def}}{=} h_0 \quad (4.47)$$

in the equatorial region,

$$|y| < y_c \overset{\text{def}}{=} \frac{1}{\beta\sqrt{ab}}, \quad (4.48)$$

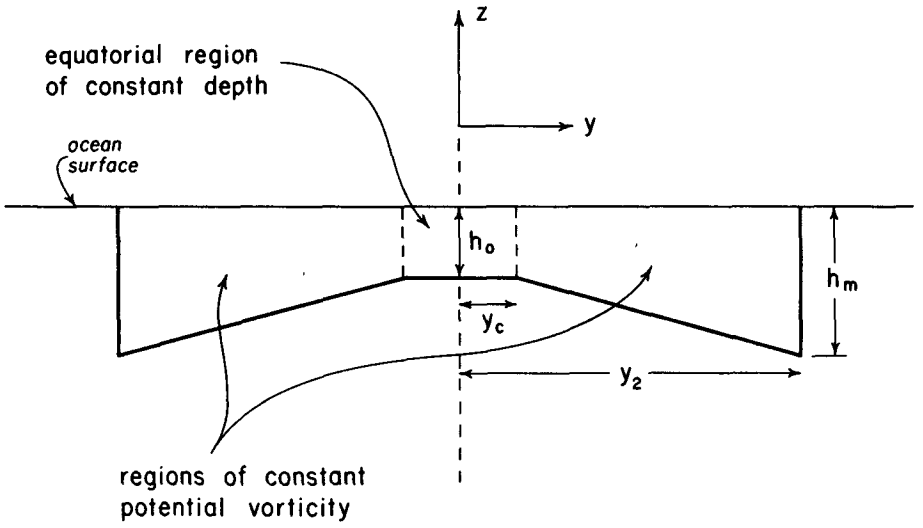

FIG. 5. The most probable thermocline shape with only mass and the simplified enstrophy $(\beta y/h)^2$ conserved.

and a nearly constant potential vorticity corresponding to

$$\langle h\rangle_\gamma \approx h_0 y/y_c \tag{4.49}$$

in the regions $|y| > y_c$. Refer to Fig. 5. To determine the most probable configuration, substitute (4.46) into (4.45) and maximize the result with respect to γ. This is in general a difficult exercise. Suppose, however, that only the subset of configurations describable by

$$y_1 < |y| < y_2 \tag{4.50}$$

is considered. The pair (y_1, y_2) replaces γ as the configuration index. The most probable of these configurations is that for which

$$\ln P_\gamma \propto \int_{y_1}^{y_2} \ln\left(\frac{\langle h\rangle_\gamma}{d}\right)dy - 2b\int_{y_1}^{y_2} \beta^2 y^2/\langle h\rangle_\gamma dy + \text{constant} \tag{4.51}$$

is maximized, where $\langle h\rangle_\gamma$ is given by (4.46). For any a, b (or equivalently h_0, y_c) the maximum of (4.51) occurs when $y_1 = 0$ and y_2 is given by

$$\ln\left(\frac{\langle h(y_2)\rangle_\gamma}{d}\right) = 2b\beta^2 y_2^2/\langle h(y_2)\rangle_\gamma. \tag{4.52}$$

The blob thus covers the equator. But if $y_2 \gg y_c$, then $\langle h(y_2)\rangle_\gamma \approx h_0 y_2/y_c$ and (4.52) implies that

$$y_2 = y_c \ln\left(\frac{h_0}{d}\right)^{1/2}. \tag{4.53}$$

The most probable thermocline is vertical at $y = \pm y_2$. It remains to choose h_0 and y_c to satisfy (4.24a) and (4.41). However, if the most probable configuration is sufficiently representative of the ensemble average, then (4.46) can be fit directly. Since the major contributions to the mass and potential enstrophy of (4.46) come from high latitude, I would determine h_0, y_c from (4.49) at the latitudinal edge (4.53) by setting

$$h_{\max} = h_0 y_{\max}/y_c \tag{4.54}$$

and

$$y_{\max} = y_c \ln(h_0/d)^{1/2}, \tag{4.55}$$

where $h_{\max}$ and $y_{\max}$ are realistic values for the maximum thermocline depth and latitude. Then as the vertical resolution increases ($d \to 0$) the ratio $y_c/y_{\max}$ decreases and the equatorial region of constant depth shrinks. In this limit, the entire blob has a *constant* potential enstrophy $\beta^2 y^2/h^2$ except for a narrow "transition region" on the equator. By filling the equatorial gridboxes "first", the blob occupies relatively many horizontal gridboxes for given total mass and potential enstrophy. The high-latitude gridboxes require a large expenditure of either h or $\beta^2 y^2/h$.

The above most probable state is unrealistic in that the thermocline attains its maximum depth at its latitudinal boundaries. As shown below, this feature disappears when the relative vorticity and total energy are properly included. However, the discontinuity in $\langle h\rangle_\gamma$ is anyway absent from the corresponding grand average $\langle h\rangle$, because the angle braces average over configurations with different y_2. The grand average is the more comparable to the nonsynoptic observations shown in Fig. 2.

I finally consider equilibrium with all three constants of motion, in the form (4.24). This calculation is much more complicated than the previous, and will be pursued only up to a point. I write h_i for

$\langle h_i \rangle_\gamma$ when no confusion can result. Again assuming that $(\partial/\partial x)\langle\ \rangle = 0$, the results of maximizing

$$S - \lambda[\sum_\gamma P_\gamma - 1] - a[\sum_\gamma P_\gamma \sum_i h_i - M_0] - b[\sum_\gamma P_\gamma \times \sum_i Z_i^\gamma - Z_0] - c[\sum_\gamma P_\gamma \sum_i E_i^\gamma - E_0] \quad (4.56)$$

are

δh_i:

$$1 = ah_i + b[2\sum_j q_j L_{ji} h_i - q_i^2 h_i] + c[h_i(\sum_j Y_{ij}h_j)^2 + 2g'h_i^2 + 2\sum_j h_j(\sum_l Y_{jl}h_l)Y_{ji}h_i], \quad (4.57)$$

δP_γ:

$$P_\gamma = Ke^{N_\gamma} \prod_i \left\{\frac{h_i}{d} \exp[-ah_i - bZ_i^\gamma - cE_i^\gamma]\right\}, \quad (4.58)$$

where

$$q_i \overset{\text{def}}{=} (\sum_j L_{ij}h_j + \beta y_i)h_i^{-1}. \quad (4.59)$$

The constants K, a, b, c are determined from (4.12) and (4.24). Multiply (4.57) by an arbitrary quantity ϕ_i and apply $\sum_i$. The result is the difference analog of

$$\int \phi dy = a\int (h\phi)dy + b\int \left[2q\frac{d}{dy}\left(\frac{g'}{\beta y}\frac{d(\phi h)}{dy}\right) - q^2\phi h\right]dy + c\int \left[h\phi\left(\frac{g'}{\beta y}\frac{dh}{dy}\right)^2 + 2g'h^2\phi + 2h\left(\frac{g'}{\beta y}\frac{dh}{dy}\right)\left(\frac{g'}{\beta y}\frac{d(h\phi)}{dy}\right)\right]dy. \quad (4.60)$$

Since (4.60) holds for any ϕ, its variation with respect to ϕ must vanish. After several integrations by parts, this leads to

$$1 = ah + b\left[2h\frac{d}{dy}\left(\frac{g'}{\beta y}\frac{dq}{dy}\right) - q^2h\right] + c\left[h\left(\frac{g'}{\beta y}\frac{dh}{dy}\right)^2 + 2g'h^2 - 2h\frac{d}{dy}\left(h\left(\frac{g'}{\beta y}\right)^2\frac{dh}{dy}\right)\right], \quad (4.61)$$

where

$$q = \left[\frac{d}{dy}\left(\frac{g'}{\beta y}\frac{dh}{dy}\right) + \beta y\right]h^{-1}. \quad (4.62)$$

Eq. (4.61) is a *nonlinear* fourth-order equation for the average thermocline depth h. The nonlinearity is the penalty paid for replacing (4.22) with (4.24). If however, I seek solutions to (4.61)–(4.62) in the restricted form

$$h = \sum_{n=0}^{\infty} H_{2n}y^{2n}, \quad q = \sum_{n=0}^{\infty} Q_{2n+1}y^{2n+1}, \quad (4.63)$$

then direct substitution of (4.63) into (4.61)–(4.62) formally determines the H_{2n} for $n > 1$, and the Q_{2n+1} for all n, in terms of H_0 and H_2, which are the arbitrary constants. The physical justification for (4.63b) is that q is an approximation to a quantity that is conserved on particles, and cannot therefore develop singularities if none are present at the initial time. The quartic truncation to (4.63a) turns out to be

$$h = H_0 + H_2y^2 + \left[-\frac{\beta^2}{8g'} + \frac{2c}{b}H_0^2H_2\right]y^4. \quad (4.64)$$

If $c = 0$ (no energy constraint) then (4.64) is identical to the quartic solution (1.6) of Section 1, and hence corresponds to potential vorticity everywhere zero. If however b, c, $H_2 > 0$, as expected, then the blob reaches higher latitude, and (4.64) resembles the compromise described heuristically in Section 1 between the tendency toward uniform q and the constraint to conserve energy. This justifies the remarks made in Section 1.

It is obvious that H_0, H_2 and c/b can be chosen to fit (4.64) to the general observations quoted at the beginning of the paper. However, in the present context a, b, c are to be fit to the mass, potential enstrophy and energy; but H_0 and H_2 are determined by boundary conditions on (4.61), which have yet to be stated. Logical boundary conditions are

$$h = 0 \quad \text{at} \quad y = \pm y_2, \quad (4.65)$$

$$\frac{d}{dy}\left(\frac{g'}{\beta y}\frac{dh}{dy}\right) + \beta y = 0 \quad \text{at} \quad y = \pm y_2, \quad (4.66)$$

where y_2 is the northern boundary of the blob (which again replaces γ as the configuration index). The condition (4.66) keeps q finite at the blob edge. Substitution of (4.64) into (4.66) leads to $c = 0$. Therefore, the quartic truncation (4.64) of (4.63a) is in general an insufficient approximation to the full solution, and higher powers of y should be included.

Suppose then that terms up to y^6 are kept so that

$$h \approx H_0 + H_2y^2 + H_4y^4 + H_6y^6, \quad (4.67)$$

where H_4 is the same as in (4.64) and H_6 is a lengthier but well-determined expression depending on a, b, c, H_0 and H_2. Substitution of (4.67) into (4.66) leads to

$$H_6 = -\frac{2}{3}\frac{c}{b}\frac{H_0^2H_2}{y_2^2} < 0, \quad (4.68)$$

so that (again assuming b, c, $H_2 > 0$) the last term in (4.67) *increases* the thermocline slope near y_2 from its value in the quartic truncation (4.64). The corresponding potential vorticity is

$$q = Q_1 y + Q_3 y^3, \tag{4.69}$$

where

$$Q_1 = \frac{2c}{b}\left(\frac{g'}{\beta}\right)H_0 H_2 > 0,$$

$$Q_3 = -\frac{c}{b}\left(\frac{g'}{\beta}\right)\left[\frac{16H_0H_2}{y_2^2} + 2H_2^2\right] < 0.$$

If $c = 0$ (no energy constraint), I still have $q \equiv 0$. However, if $c \neq 0$, q varies linearly with latitude near the equator $y = 0$, but then "flattens off" at higher latitudes, because Q_1 and Q_3 have opposite signs. Thus the higher truncations (4.67, 4.69) begin to resemble the simpler case of Fig. 5 in which only the simplified potential vorticity $\beta y/h$ was considered. Apparently, a principle role of the energy constraint is to keep the relative vorticity from becoming too large. The energy constraint can perhaps sometimes be dropped, but only if the relative vorticity is simultaneously dropped from the enstrophy. It is striking that the absurdly simple shape of Fig. 5 does, in fact, resemble the deeper isopycnals (1–3 km) in Fig. 2.

The principal results of this section can also be derived—somewhat more simply—by the following more heuristic approach. Suppose, *a priori*, that the blob is divided into M identical rigid bricks which can then be distributed arbitrarily over the network of N horizontal gridboxes. Let m_i be the number of bricks at the ith gridbox. The thermocline depth at the ith gridbox is proportional to m_i. A macro-state of the blob,

$$\{m_1, m_2, \ldots, m_N\}, \tag{4.70}$$

is defined by specifying the number of bricks at each of the N gridboxes. Adopt Boltzmann's definition of the entropy,

$$S = \ln W, \tag{4.71}$$

where

$$W = \frac{M!}{m_1!m_2! \cdots m_N!} \tag{4.72}$$

is the number of ways to realize the state (4.70). The numerator of (4.72) recognizes that each state (4.70) is unaltered by the $M!$ possible permutations of the bricks. However, permutations of bricks within the same gridbox should not be counted, because there is no way to distinguish between identical bricks at the same location. The denominator of (4.72) corrects for this over-counting. Replacing[7]

$$\ln(m_i!) \approx m_i \ln m_i \tag{4.73}$$

and then maximizing S subject to the conservation of mass,

$$\sum_i m_i = M, \tag{4.74}$$

and potential enstrophy,

$$\sum_i \beta^2 y_i^2/m_i = Z, \tag{4.75}$$

leads to the analog of (4.44), namely,

$$\ln m_i = a - b\beta^2 y_i^2/m_i^2. \tag{4.76}$$

The solutions to (4.76) are qualitatively similar to those of (4.44), and there is now no need to average over γ. I call this approach heuristic because it is not obvious how to construct a truncated dynamics (possessing the Liouville property) in which massive fluid parcels remain localized in physical space. The more general method given above avoids this difficulty. Moreover, since the general method addresses the full probability distribution in phase space, it can (in principle) furnish *any* equilibrium flow statistic.

5. Dynamics of the blob

Numerical experiments described in this section confirm that the unforced blob assumes the double-lobe shape spontaneously. The experiments also reveal the *mechanism* of adjustment, which absolute equilibrium theory cannot address. No statistical hypotheses are required here, and in fact almost none of the special assumptions of Section 4 are invoked.

I continue to consider the equivalent barotropic model with Lagrangian (4.4). As previously stated, independent variations $\delta x(a, b, \tau)$ and $\delta y(a, b, \tau)$ of (4.4) yield the momentum equations (4.2ab). It is now however convenient to define conjugate momenta

$$\frac{\delta L}{\delta\left(\frac{\partial x}{\partial \tau}\right)} = \rho_0 u \quad \text{and} \quad \frac{\delta L}{\delta\left(\frac{\partial y}{\partial \tau}\right)} = \rho_0 v, \tag{5.1}$$

and to invoke Hamilton's principle in the "extended" form,

$$\frac{\delta}{\delta x}, \frac{\delta}{\delta y}, \frac{\delta}{\delta u}, \frac{\delta}{\delta v}\left[\int L d\tau\right] = 0, \tag{5.2}$$

where now

$$L = \tfrac{1}{2}\rho_0 \iint dadb\left[u\frac{\partial x}{\partial \tau} + v\frac{\partial y}{\partial \tau} - \mathscr{H}\right] \tag{5.3}$$

and $\mathscr{H}$ is the Hamiltonian density (defined below). It is also convenient, for reasons of computation, to replace the mass labeling coordinates (a, b) with new coordinates (x_0, y_0) which are the (x, y) position coordinates of the fluid particles at some labeling time τ_0. Then Hamilton's principle is just (5.2) with x, y, u, v considered as functions of (x_0, y_0, τ), and

[7] The approximation (4.73) is accurate for large m_i, and may therefore be inappropriate near the blob edges. It is however well-behaved for all integers m_i.

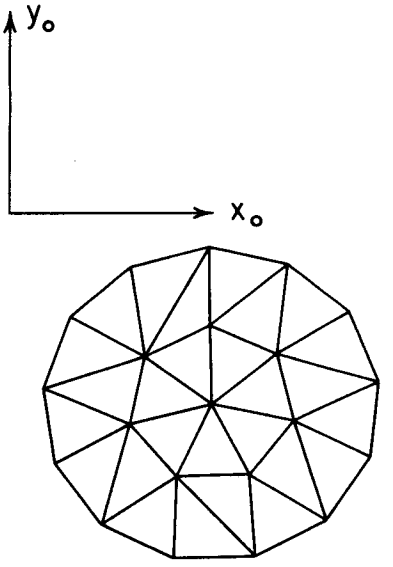

FIG. 6. The finite element grid in labeling space.

$$L = \iint dx_0 dy_0 h^0 \times \left[u \frac{\partial x}{\partial \tau} + v \frac{\partial y}{\partial \tau} - \beta y^2 \frac{\partial x}{\partial \tau} - \mathscr{H} \right], \quad (5.4)$$

where

$$\mathscr{H} = \tfrac{1}{2}(u^2 + v^2) + \tfrac{1}{2} g' h^0 \frac{\partial(x_0, y_0)}{\partial(x, y)}. \quad (5.5)$$

Here

$$h^0 \overset{\text{def}}{=} \frac{\partial(a, b)}{\partial(x_0, y_0)} = h^0(x_0, y_0) \quad (5.6)$$

is the thermocline depth at the labeling time τ_0 and

$$h \overset{\text{def}}{=} h^0 \frac{\partial(x_0, y_0)}{\partial(x, y)} = h(x_0, y_0, \tau) \quad (5.7)$$

is the actual thermocline depth at time τ. The independent variations δx, δy, δu, δv now yield (4.2ab) and

$$\frac{\partial x}{\partial \tau} = u, \quad \frac{\partial y}{\partial \tau} = v. \quad (5.8)$$

As before, the mass conservation equation (4.2c) is a direct consequence of the definitions (5.6) and (5.7).

The Lagrangian formulation is appropriate because the blob occupies a region of (x_0, y_0) space whose boundaries are fixed in time. Let this region be covered with triangular finite elements as shown in Fig. 6. The triangle vertices are called nodes, and the dependent variables of the numerical model are just the values of x, y, u, v at each of the nodes. Within each element, the variables h^0, x, y, u, v are assumed to be linear interpolates of the three nodal values. Concisely,

$$x(x_0, y_0, \tau) = \sum_i x_i(\tau) N_i(x_0, y_0) \quad (5.9)$$

(plus similar equations for h^0, y, u, v) where $x_i(\tau)$ is the value of x at the ith node and the summation runs over all nodes. The "shape function" $N_i(x_0, y_0)$ is nonzero only within elements sharing the ith node, and there it takes the value

$$N_i(x_0, y_0) = A_i/(A_i + A_j + A_k), \quad (5.10)$$

where A_i, A_j, A_k are the areas of the regions shown in Fig. 7. Substitution of (5.9) and its counterparts brings the Lagrangian (5.4) into the form

$$L = \sum_{i,j,k} [u_i \dot{x}_j + v_i \dot{y}_j - \tfrac{1}{2} u_i u_j - \tfrac{1}{2} v_i v_j] h^0_k \iint dx_0 dy_0 \times N_i N_j N_k - \beta \sum_{i,j,k,l} y_i y_j \dot{x}_k h^0_l \iint dx_0 dy_0 N_i N_j N_k N_l - \tfrac{1}{2} g' \iint dx_0 dy_0 \left[\sum_{i,j} h^0_i h^0_j N_i N_j / \sum_{i,j} x_i y_j \frac{\partial(N_i, N_j)}{\partial(x_0, y_0)} \right]. \quad (5.11)$$

The $dx_0 dy_0$ integrals in (5.11) are easily computed constant factors. [Note that $\partial(N_i, N_j)/\partial(x_0, y_0)$ is piecewise constant over every element.] Thus (5.11) is any ordinary function of the variables $\{x_i(\tau), y_i(\tau), u_i(\tau), v_i(\tau)\}$. The numerical dynamics result from Hamilton's principle in the form

$$\frac{\delta}{\delta x_i}, \frac{\delta}{\delta y_i}, \frac{\delta}{\delta u_i}, \frac{\delta}{\delta v_i} \left[\int L d\tau \right] = 0, \quad \text{all } i. \quad (5.12)$$

The finite element form of

$$\iint \mathscr{H} h^0 dx_0 dy_0$$

is automatically conserved.

At the labeling time τ_0, (x_0, y_0) coincides with true particle location (x, y) and the element boundaries in (x, y) are, by design, nearly equilateral triangles. As time increases, however, the fluid motion strains the elements into long thin triangles in (x, y) space, and numerical accuracy erodes. Occasionally, therefore, the fluid particles must be re-labeled and the elements entirely redrawn, keeping the depth and

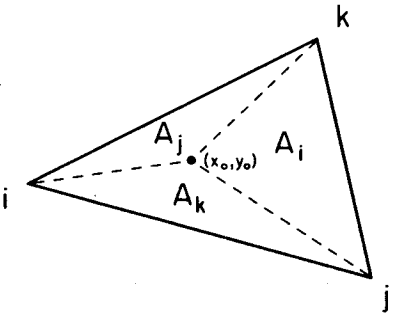

FIG. 7. A single element. For an explanation, see the text.

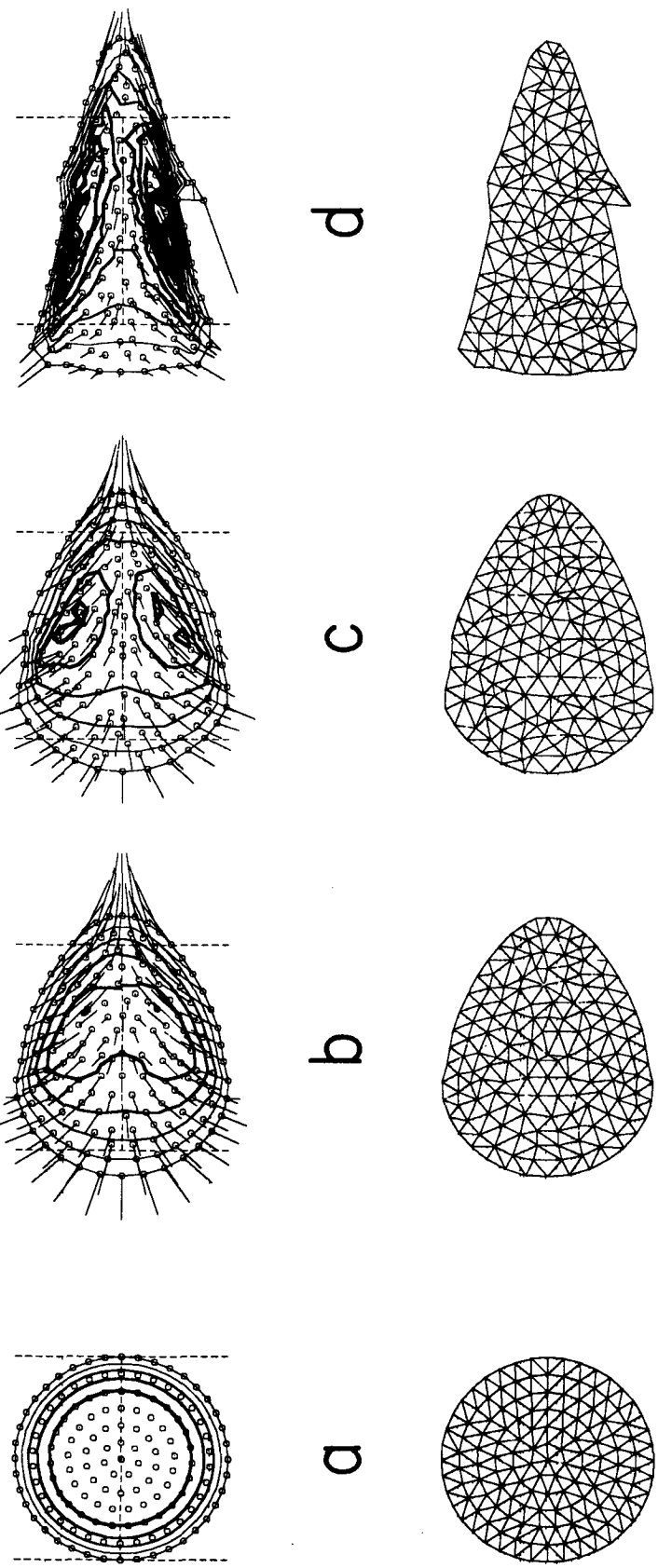

FIG. 8. The time evolution of the blob in experiment A. The horizontal dashed line is the equator. The small circles are fluid particles located at the nodes. Closed solid lines are thermocline depth contours with 100 m intervals. Darker lines denote deeper thermocline. The straight lines emanating from the fluid particles are instantaneous velocity vectors. The blob is shown at (a) 0 days, state of rest; (b) 35 days; rms velocity 17.4 cm s^{-1}; (c) 50 days; 18.3 cm s^{-1}; (d) 157 days; 19.4 cm s^{-1}.

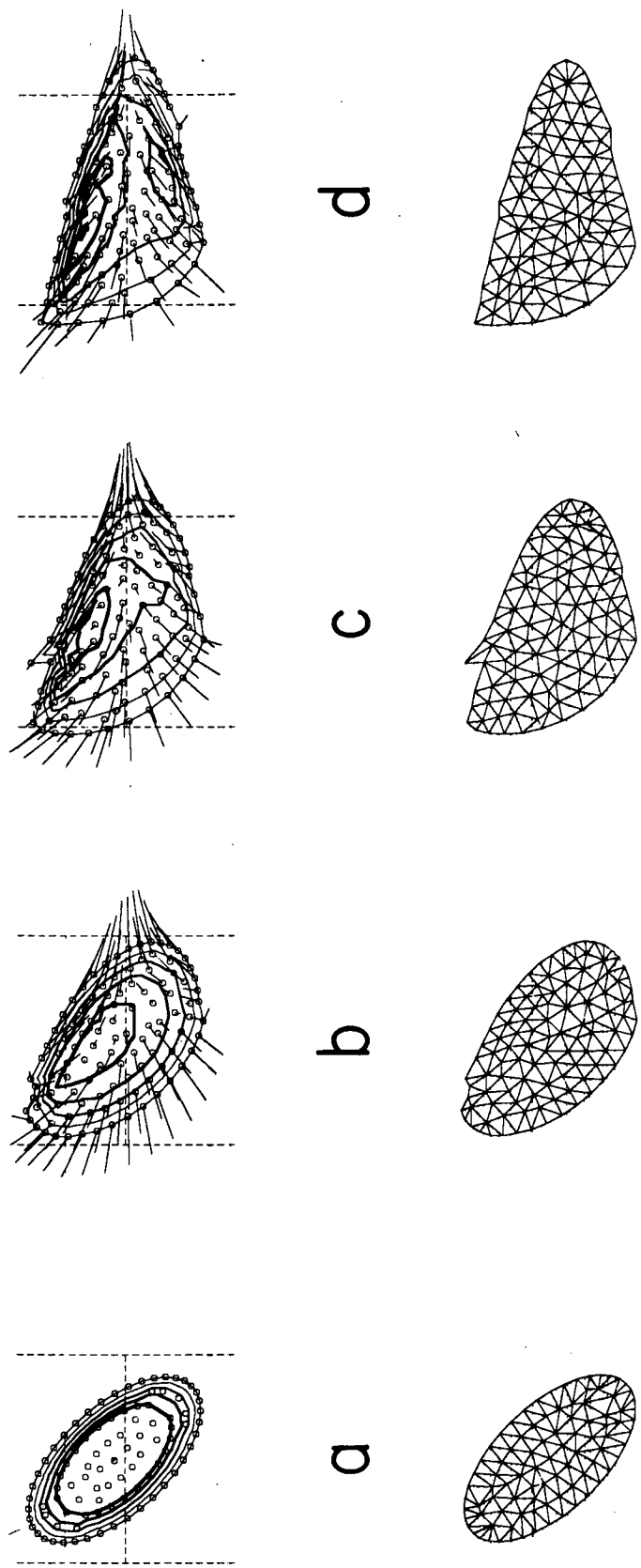

FIG. 9. As in Fig. 8 except for experiment B at (a) 0 days; state of rest; (b) 17 days; 23.5 cm s^{-1}; (c) 52 days; 18.3 cm s^{-1}; (d) 87 days; 17.5 cm s^{-1}.

velocity fields and the blob boundary unchanged. The new element grid consists of nearly equilateral triangles of uniform size. In the experiments discussed, particles were re-labeled about every 50 time steps.

I describe two experiments, corresponding to the initial conditions shown in Figs. 8a and 9a. In experiment A the initial blob is a lens of radius 5000 km and maximum depth 500 m centered on the equator. In experiment B, the blob is initially a skewed ellipse with maximum depth 500 m centered 500 km north of the equator. In Figs. 8 and 9, the horizontal coordinates are "true location" (x, y); the nodes, shown as small circles, can be considered marked fluid particles; the closed solid lines are h contours with 100 m interval; and the straight lines emanating from particles are instantaneous velocity vectors. In both experiments the blob is contained between east and west "rubber coastlines," which are introduced by adding the potential

$$V(x) = (50 \text{ cm s}^{-1})^2\left(\frac{x}{1000 \text{ km}}\right)^2 \qquad (5.13)$$

to the right side of (5.5). This potential provides a restoring force which keeps the blob from spreading out indefinitely along the equator. I have also added a simple quadratic friction in the form

$$\frac{\partial \mathbf{u}}{\partial \tau} = \text{previous terms} - (0.05 \text{ km}^{-1})|\mathbf{u}|\mathbf{u}. \qquad (5.14)$$

Although *zero* friction would better match the hypotheses of previous sections, the large kinetic energy which results is difficult to handle numerically. Again, the numerical experiments are not intended as a precise check on the absolute equilibrium theory. Rather, the experiments show that the conclusions of the equilibrium theory are qualitatively correct even without the restrictive assumptions of Section 4.

Figs. 8 and 9 show the time evolution of the blob in experiments A and B. In both experiments, geostrophic currents rapidly develop in the sense expected from the isopycnal slopes. The flow is strong enough to carry particles all the way around the blob in several months. The geostrophic currents cause mass divergence in the western equatorial blob and convergence in the eastern equatorial region. The divergence reduces the thermocline depth, and this shoaling gradually migrates from west to east along the equator, dividing the blob into two deep extratropical lobes. The initial asymmetry in experiment B persists, but the blob still separates into two lobes. Also as anticipated in Section 4, the thermocline slope is maximal at the north and south blob boundaries.

Figs. 10 and 11 are scatter plots of the potential vorticity q and the "Rossby parameter" (relative vorticity/planetary vorticity) for all elements in both experiments at various times. The plots show that the potential vorticity does indeed mix toward a uniform

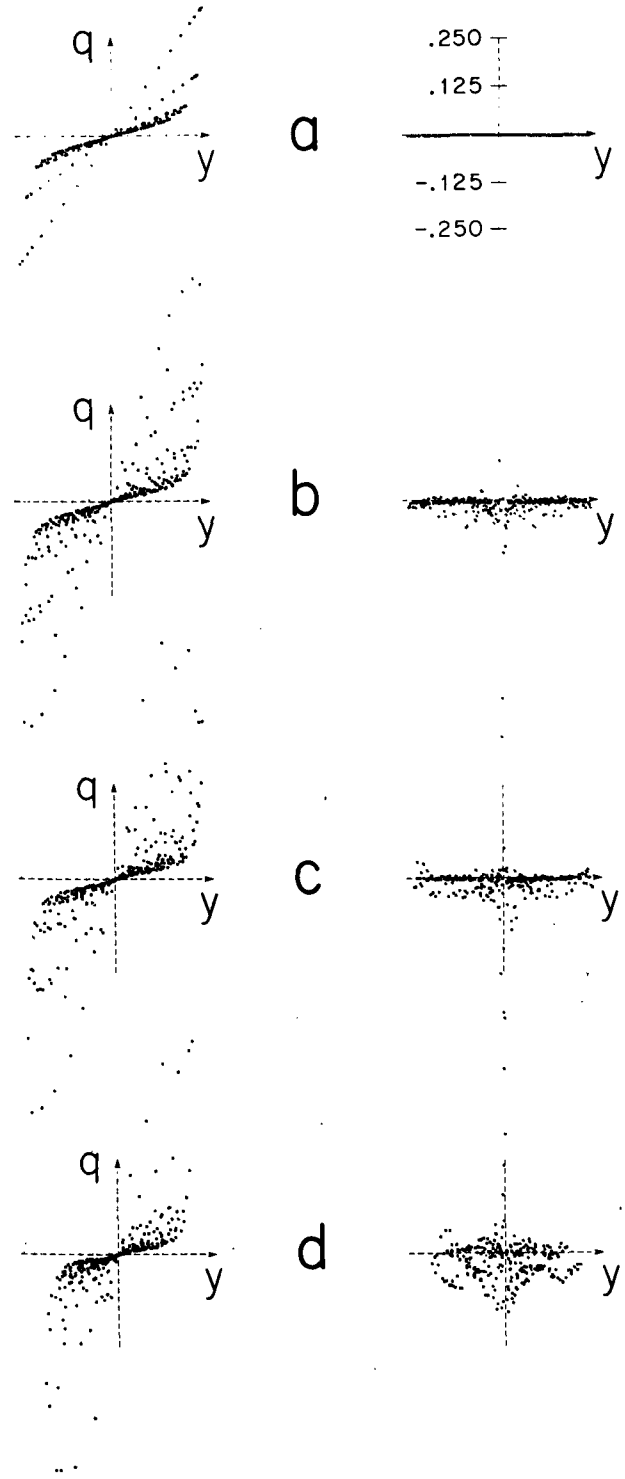

FIG. 10. The potential vorticity q (left, linear scale) and Rossby ratio, relative vorticity/planetary vorticity, (right) for each element in experiment A at (a) 0 days, (b) 35 days, (c) 50 days, (d) 157 days.

average outside a narrow equatorial transition region, as the theory of Section 4 would predict. If the potential vorticity were to become uniformly zero, then

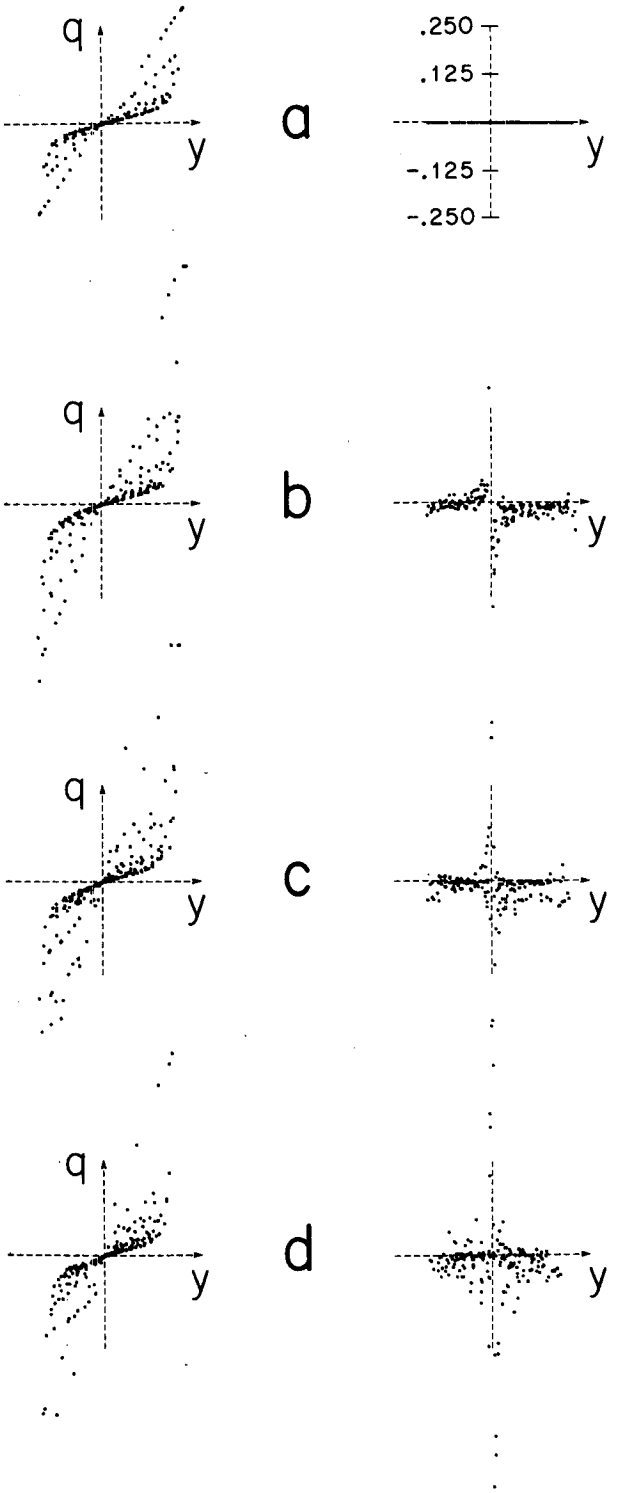

FIG. 11. As in Fig. 10 except for experiment B at (a) 0 days, (b) 17 days, (c) 52 days, (d) 87 days.

the Rossby parameter would be minus unity. Both the friction and energy conservation resist this, but the plots definitely show a uniform tendency toward negative Rossby parameter. The overall adjustment is rapid because the rms fluid velocity is large (20 cm s^{-1}). Smaller friction hastens the adjustment, but the end state is qualitatively similar.

6. Remarks

I have argued that the observed mean ocean density field resembles the state of maximum entropy for given values of the mass, potential enstrophy and energy. If the energy constraint is dropped, these maximum entropy states exhibit hemispheric regions of uniform potential vorticity. In this sense, the equilibrium states may be understood heuristically as the states of most uniform average potential vorticity that energy conservation will allow. To the extent these results apply to reality, the wind and thermal forcing are important only as the sources of total energy, potential enstrophy and water type. The gross isopycnal shape would be the same if the winds reversed, or if some agency other than wind were the source of excitation. The simplicity of this viewpoint, which rests on only the most elementary conservation laws and the hypothesis of mixing in phase space, is the most noteworthy result of this work.

Recently, Rhines and Young (1982a,b) have suggested that down-gradient mixing of mean potential vorticity by eddies is an important phenomenon which explains large regions of uniform potential vorticity in real and numerical oceans. They adopt quasi-geostrophic dynamics, which take the mean stratification as given. I suggest that the mean density field itself is the result of potential vorticity mixing. The mixing proceeds against the restraining effect of energy conservation.

The inviscid equilibrium flow of a single-layer ocean in a rectangular beta-plane basin has been discussed by Salmon (1982). The mean streamfunction obeys the same equation considered by Fofonoff (1954), namely,

$$\nabla^2\psi + \beta(y - y_0) = (a/b)\psi,$$

where a and b are the Lagrange multipliers corresponding to the energy and potential enstrophy. Again, if the energy constraint is dropped ($a = 0$), the mean potential vorticity is uniform, but the equilibrium energy is unrealistically large. For realistically small initial energy, $l \equiv (b/a)^{1/2}$ is much smaller than the basin size, and inertial boundary layers of thickness l close a uniform westward interior flow. The equilibrium mean flow in a multi-layer quasi-geostrophic ocean is nearly barotropic and substantially the same: the strong inertial currents are still confined to boundary layers. However, in the equilibria of this paper, which are the analogs of Fofonoff's solution for a completely free upper layer, the strong inertial currents occur at the blob boundary, in mid-ocean. These results collectively suggest that a quasi-geo-

strophic western boundary current will not readily separate from the coast without essential help from forcing and friction. However, if the thermocline is free to surface, then boundary layer separation can occur spontaneously.

Acknowledgments. I am supported by the National Science Foundation. This project was begun while I was a visitor at the Aspen Center for Physics.

REFERENCES

Bretherton, F. P., 1970: A note on Hamilton's principle for perfect fluids. *J. Fluid Mech.*, **44,** 19–31.

Carnevale, G. F., 1982: Statistical features of the evolution of two-dimensional turbulence. *J. Fluid Mech.*, **122,** 143–153.

——, U. Frisch and R. Salmon, 1981: H theorems in statistical fluid dynamics. *J. Phys.*, **A14,** 1701–1718.

Eckart, C., 1960: Variation principles of hydrodynamics. *Phys. Fluids*, **3,** 421–427.

Fofonoff, N. P., 1954: Steady flow in a frictionless homogeneous ocean. *J. Mar. Res.*, **13,** 254–262.

Fox, D. G., and S. A. Orszag, 1973: Inviscid dynamics of two-dimensional turbulence. *Phys. Fluids*, **16,** 169–171.

Hopf, E., 1952: Statistical hydromechanics and functional calculus. *J. Rat. Mech.*, **1,** 87–123.

Jaynes, E. T., 1957: Information theory and statistical mechanics. *Phys. Rev.*, **106,** 620–630.

Katz, A., 1967: *Principles of Statistical Mechanics: The Information Theory Approach.* W. H. Freeman, 188 pp.

Kells, L. C., and S. A. Orszag, 1978: Randomness of low-order models of two-dimensional inviscid dynamics. *Phys. Fluids*, **21,** 162–168.

Kraichnan, R. H., 1975: Statistical dynamics of two-dimensional flow. *J. Fluid Mech.*, **67,** 155–178.

——, and D. Montgomery, 1980: Two-dimensional turbulence. *Rep. Prog. Phys.*, **43,** 547–619.

Lee, T. D., 1952: On some statistical properties of hydrodynamical and magneto-hydrodynamical fluids. *Quart. J. Appl. Math.*, **10,** 69–74.

Lynn, R. J., and J. L. Reid, 1968: Characteristics and circulation of deep and abyssal waters. *Deep Sea Res.*, **15,** 577–598.

Onsager, L., 1949: Statistical hydrodynamics. *Nuovo Cimento Suppl.*, 9, **6,** 279–287.

Rhines, P. B., and W. R. Young, 1982a: Homogenization of potential vorticity in planetary gyres. *J. Fluid Mech.*, **122,** 347–367.

——, and ——, 1982b: A theory of the wind-driven circulation. *J. Mar. Res., Suppl.*, **40,** 559–596.

Ripa, P., 1981: Symmetries and conservation laws for internal gravity waves. *Amer. Inst. Phys. Proc.*, **76,** 281–306.

Salmon, R., 1982: Hamilton's principle and Ertel's theorem. *Amer. Inst. Phys. Proc.*, **88,** 127–136.

——, 1982: Geostrophic turbulence. *Proc. Int. School of Physics Enrico Fermi.* Varenna, Italy, 30–78.